The ionization loss of fast cosmic ray -mesons at ground level

R. H. West

ABSTRACT

THE IONIZATION LOSS OF FAST COSMIC RAY MU MESONS AT GROUND LEVEL.

A review is made of the theoretical and experimental methods relating to
the measurement of energy loss by ionization of fast charged particles on
passing through a medium. A detailed account of the problems arising when the
medium is a gas is given together with reasons for preferring the use of a
proportional to measure the energy loss.

As a pro portional counter is considered to be best used to
measure the most probable energy loss a discussion of the relevant theory
is included in the review.

In addition to the review an experiment designed to measure the
rate of energy loss of fast cosmic ray mesons and the variation of this rate
with the total energy of the particle is reported. This experiment has two functions ;
to elucidate some of the problems arising in the theoretical discussion, and
to determine the optimum experimental conditions for a more extended experiment.

Cosmic ray mesons are a convenient source of particles of the required
energy (1-100 Gev), and, within this energy range, relatively uncontaminated.
However as a result of the wide energy spectrum of the mesons the energy of each
particle used must be measured. This is best done using a magnetic spectrograph,
and such an instrument and its use are described.

The results of the experiment are given together with those of other
work in this field and compared with theory. They show that the general theory is
broadly correct but the experiments are not accurate enough to distinguish between
the more refined theories.

Finally, suggestions are made concerning an improved experiment
of the type described.

THE IONIZATION LOSS OF FAST COSMIC RAY μ-MESONS

AT GROUND LEVEL.

A Thesis submitted to the University of Durham

for the degree of Master of Science

by

R.H.West B.Sc..

December 1962.

PREFACE.

This thesis describes the use of proportional counters in conjunction with the Durham High Energy Cosmic Ray Spectrograph to measure the most probable ionization energy loss of relatioistic u-mesons in a neon methane mixture.

The experiment was initiated by D.G. Jones who constructed most of the equipment and obtained the initial results. The authors task was to examine the theoretical work in this field and relate it to the experiment and also to continue with the experimental work with a view to determining the optimum conditions for such an experiment.

In the course of this investigation additional results were obtained, which together with those of Jones give an accurate measurement of the variation of ionization energy loss with the total energy of the u meson in the range from below 1 Gev to above 10 Gev.

This work was carried out at the Physics Department of the Durham Colleges in the University of Durham under the supervision of Dr. A.W. Wolfendale during the year 1959-60.

CONTENTS.

CHAPTER 1

INTRODUCTION

When a charged particle passes through matter it loses energy by two processes, other than nuclear interaction, both due to collisions with the fundamental constituents of the material. One is due to energy transfers to the electrons of the material, causing ionization or excitation of the atoms, and the other to radiative losses when the particle is scattered. The latter is often termed 'bremsstrahlung'. The work to be described concerns only ionization and excitation losses, radiation losses are of importance only at energies higher than those in which we are interested.

1.1 Average Energy Loss

It will be convenient to use the term 'ionization loss' to cover both energy transfers causing ionization and those causing excitation. The simple classical theory of ionization loss is due to Bohr (1915) and is based on the concept of a free electron experiencing an impulsive force due to the nearby passage of the charged particle and its associated field. This has been extended to cover incident particles having relativistic

energies, where the pulse received by the electron is sharpened and intensified by Lorentzian contraction of the field. The result is an increase in rate of energy loss at energies above about 3.5 times the rest energy.

Such a treatment, using more accurate cross sections was made by Bethe (1932, 1933). It was then pointed out by Swann (1938), and calculated first by Fermi (1939, 1940), that polarization of the medium would reduce the effect of the energetic particles' field. Thus the increase in energy loss would not be as great as that predicted by the Bethe formula. Fermi, and later workers, then showed that a 'plateau' should be reached at an energy dependent on the material and the density of that material.

A typical curve of ionization loss against energy is shown in Fig. 1. The curve may be divided into four regions:

    I Classical: velocity^{-2} dependence

    II Minimum

    III The 'log rise'

    IV The Fermi plateau.

The graph given in Fig. 1 refers to $\frac{dE}{dx}$, the average energy loss per unit path length, but in fact the loss of energy is not a continuous process, a discrete amount

being lost at each collision. These collisions may be divided into two abitrary classes: close and distant, depending on the closest distance of approach of the energetic particle (the impact parameter). The distant collisions are frequent and the energy loss per colli- sion relatively small whereas the few close collisions each involve a large energy transfer. Thus, for the energy lost in a thin film, we should not expect to find a constant value but a distribution about the mean predicted by the energy loss equation. The effect of different rates for close and distant collisions leads to a skew distribution, of the form shown in Fig. 2 where the approximate contributions due to the two types are indicated.

1.2 Primary and Secondary Ionization

The ions produced by the initial collision of the traversing particle form the 'primary ionization'. Some of these ions may have sufficient energy to cause further ionization themselves; this is the 'secondary ionization'.

1.3 Most Probable Energy Loss

Fig. 2 introduces the concept of the most probable energy loss, defined as the loss for which the distribu- tion has its maximum. This is less than the average
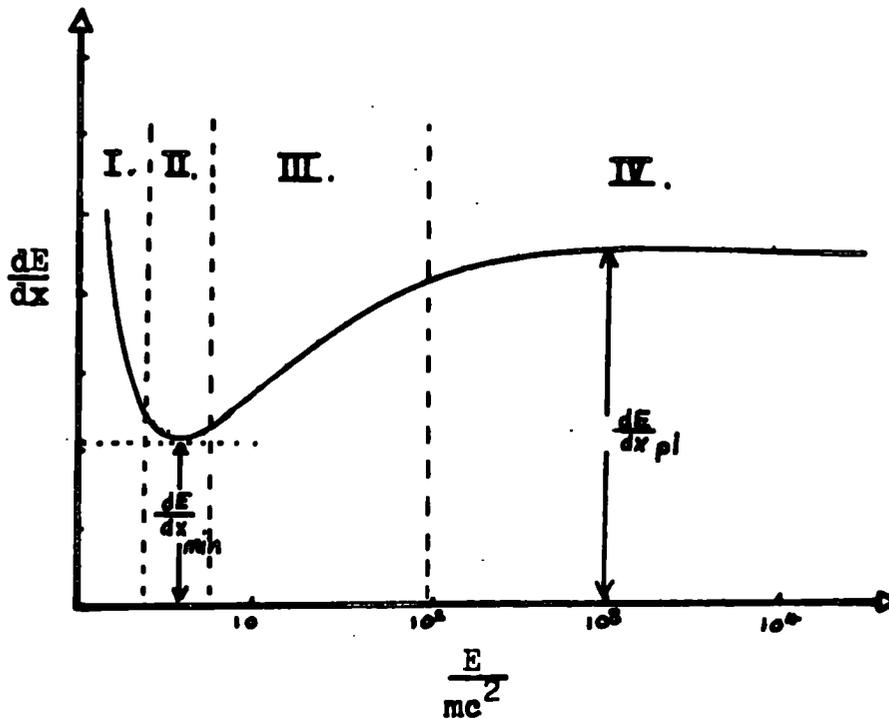
Fig. 1. Typical Ionization Loss Relationship.
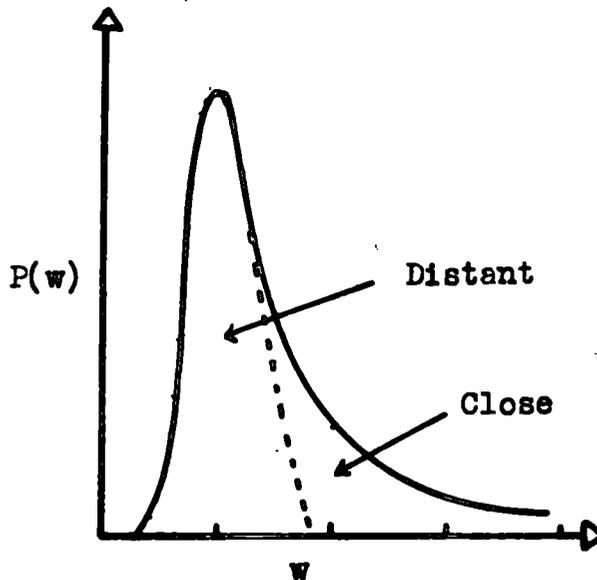
Fig. 2. Probability $P(w)$ of an Energy Loss w in a thin Absorber.

energy loss and will not be far removed from the average energy loss for distant collisions.

1.4 Methods of Measurement of Energy Loss

The formation of ions by a moving charged particle forms the basis of nearly all particle detectors. Conversely, nearly all of these detectors may be used to measure the amount of ionization produced by the particle and hence the energy loss. Two assumptions are inherent in the method, firstly, that the ionization measured is proportional to the ionization energy loss, which includes excitation and, secondly, that the energy loss per ion pair is dependent neither on the type of charged particle nor on its energy. The implications of these assumptions and where possible the justifications for them will be discussed in Chapter 6.

Alternatively, the energies of a particle before and after traversing an absorber of known thickness may be measured, from which the energy loss may be calculated. For accuracy the energy loss would not have to be small compared with the initial energy. This would lead to difficulties in comparing results with theory, since we would expect the rate of energy loss to change in such a thick absorber. Nevertheless the method has been used by some workers.

Methods by which energy loss may be measured have been comprehensively reviewed by Price (1955) and only brief comment will be made here.

The methods may be classified as in Fig. 3.

In this work interest is centred on the 'log rise' region. We may then disregard all methods using energy loss in a condensed medium, since the onset of the density effect at lower energies than for gases will shorten the 'log rise' region. It was this fact which lead many earlier workers in this field, using solid or liquid detectors to report an absence of log rise.

The gaseous detectors will now be considered.

The Cloud Chamber

A cloud chamber may be used in two ways, depending on the time between the passage of the particle and the expansion of the chamber. If the expansion takes place immediately the secondary ions will not have had time to diffuse away from the vicinity of the primary ion, and the resultant drop count will give a measure of the primary ionization.

Delaying the expansion will allow the secondary ions to diffuse and each will form a separate drop. Here again there are two courses open on analysis of the drop counts. Either the most probable number may be measured or the

Particle Detectors (measurement of the rate of energy loss in the detector)	Gaseous	Cloud Chamber Ionization Chamber Proportional Chamber Low Pressure Geiger Counter
	Condensed	Emulsions Scintillators Semiconductors
Measurement of $E_{in} - E_{out}$ for a particle passing through an absorber		Electron in Metallic Films Magnet-cloud chamber with plates Cosmic Rays in the Earth

Fig. 3 Methods of Measuring Energy Loss.

average number excluding large drop clusters. These two values, differing in concept, may not differ greatly in magnitude, depending on the value of the cut-off. The theory for this latter method is quoted by Sternheimer (1953).

The apparent advantage of the cloud chamber method is that both alternatives may be compared directly with theory, although the author feels that the theory for most probable energy loss cannot be regarded as basic (Chapter 7).

Against this are the considerable difficulties of operation, especially in the precision required in the conditions for condensation, affecting the fraction of ions which will act as nuclei. Cloud chambers are usually used with a clearing field to diffuse the secondary ions when it is possible to get conditions such that all of the positive ions will act as condensation nuclei (Price 1955).

In his review Price concludes that the best way of using the cloud chamber is to measure the most probable ionization. This quantity is measured more easily using a proportional counter, however, and the advantage of using a cloud chamber is lost.

Finally, although, with the cloud chamber, ionization measurements are quite capable of distinguishing between different particles of comparable energy when their energy is low (Fig. 1 Region I),

t̶T̶he resolution of relativistic particles is very difficult since individual ionization estimates commonly have uncertainties of some tens of per cent.

The Proportional Counter

The proportional counter may be used to determine the most probable ionization only for several reasons. Firstly large energy transfers produce such large pulses that the associated amplifiers will be saturated. A more important point, however, is that some of the large energy transfers will be due to low energy electrons knocked out of the walls of the counter i.e. they will not correspond to energy transfers within the gas of the counter. Nevertheless the improvements in linearity and stability of modern amplifiers and associated equipment, and the fact that the stability of the counter and its equipment may be calibrated by the use of suitable X-ray sources, are strong arguments in favour of the use of proportional counters.

Low Pressure Geiger Counters

If the pressure inside a geiger counter is reduced so that the chance of a particle producing an ion pair is small, then the counter can be used to determine the number of ionizing collisions.

This requires that the counter be sensitive to one ion pair and also that there are no knock-on electrons emerging from the walls into the gas. The first condition may be satisfied using gases with low attachment coefficients and it has been shown that the effect of knock-on electrons is small enough not to be serious.

Thus the primary ionization may be measured in this way. The measurements should not be subject to the large fluctuations of the results from the proportional counter, since there the variations are due not so much to the fluctuations in number of primary events, but to the differing amounts of secondary ionization that may be produced.

Although an interesting method, it is again a difficult one and if μ-mesons, and hence cosmic rays, are to be used the rate of gathering information will be very low.

1.5 The use of cosmic rays as a source of charged particles

The source of charged particles for the experiments to be described was the cosmic radiation and some discussion of these particles is required. The radiation falling on top of the earth's atmosphere has been shown to consist of approximately 90% protons, the rest being heavier nuclei, mainly alpha particles. As they enter the atmosphere these heavier nuclei disintegrate. The protons interact with air nuclei to produce charged and uncharged π and K-mesons predominate. Although these will be produced throughout the atmosphere the production spectrum falls off steeply with depth and it is sufficiently accurate for our purposes to assume that all the π -mesons are produced in the first 200 gm cm^{-2} of the atmosphere (total thickness $\sim$ 1000 gm cm^{-2}). The $\pi^{\pm}$ - mesons have a lifetime of 2.6 x 10^{-8} sec and decay into μ-mesons. The μ-mesons have a much weaker interaction with matter and as their lifetime is comparatively long (2.2 x 10^{-6} sec) many survive to sea level, losing approximately 2 GeV of energy through the atmosphere. The π^{0} mesons produced by the primary protons decay into γ-rays almost immediately (lifetime 10^{-16} secs). These materealise into high energy electron pairs which in turn

emit γ-rays (bramsstrahlung), and give rise to the electron-photon cascade phenomenon.

Thus, arriving at sea level, there are two components of cosmic rays usually referred to as the hard and soft components. The hard component consists of μ-mesons with about 1% protons, and the soft component is composed of electrons and slow μ-mesons. There is also a small flux of neutrons and a very few π-mesons. We may easily filter off the soft component and since we are only interested in charged particles we will then have a μ-meson. source with proton contamination. The proton spectrum, measured by Mylroi and Wilson (1950) shows that the protons have mainly an energy less than 1 GeV and virtually all have energies below 10 GeV. Thus the majority of the protons will fall in the $\frac{1}{v}2$ region of the ionization curve and have a high energy loss which will not affect the measurement of the most probable energy loss of the μ-mesons.

1.6 Energy range of μ-mesons required

The minimum ionization loss occurs for -mesons with momenta about 0.4 GeV/c and the commencement of the transition from the log rise to the plateau is at momenta $>$15 GeV/c, the exact value depending on the density and nature of the gas in which the ionization is being

measured. To have a measurement well on the plateau,

one at 100 GeV/c is desirable. The only type of momentum

measuring instrument that will include this value within

its range of measurement is a magnetic spectrograph.

1.7 A Magnetic Spectrograph

In a magnetic spectrograph the charged particle is

deflected in a magnetic field, H, acting over a distance

$\underline{1}$. If its momentum is p and the angle of deflection is θ

$$p\theta = 300 \int Hdl \qquad \qquad \ldots\ldots\ldots 1a.$$

where p is measured in eV/c.

and $\int Hdl$ is the line integral of the magnetic field along

the path of the particle in gauss-cm.

The Durham Cosmic Ray Spectrograph is capable of

measuring momenta up to 1000 $\pm$ 200 GeV/c. and is thus

quite suitable for the type of measurement discussed.

It has been used in conjunction with proportional counters

to study the variation of ionization loss of μ-mesons in

the log rise region. The present work examines the

requirements for a successful experiment of this nature

and describes some preliminary results.

There has been previous work using cosmic ray μ-

mesons and it has been established that a log rise of

the order predicted by theory does occur, yet there are

few experiments which include results both below the

minimum and on the plateau. The transition region to the plateau is particularly lacking in accuracy and no experiment has been able to distinguish between the more refined theories for these momenta.

CHAPTER 2

THE DURHAM SPECTROGRAPH

2.1 The Instrument

The Durham Spectrograph is shown diagrammatically in Fig. 4. The magnet is of the type used in the Manchester spectrograph (Hyams et al 1950), and has a field volume, in air, of 40 cm x 30 cm x 15 cm. When operated at a current of 60 amps the line integral of the magnetic field is $\int Hdl = 6.2 \times 10^5$ gauss-cm.

The particles to be measured are required to give a five-fold coincidence between the geiger counters in trays A, B, C, D and the gap counters, G. The three counters in the gap, G, ensure that the particle selected does not pass through the iron of the magnet.

It is simpler, experimentally, not to measure the angle of deflection of the particle in the instrument but the horizontal deflection, Δ, for a known 'arm' d.

We then have $p = \dfrac{300\ d \int Hdl}{\Delta}$, by substituting $\theta = \Delta/d$ in equation 1. In the equation Δ and d are expressed in cm. and p is in eV/c.

	5.5 cm. Lead
	25 G.M.
	944 Flash Tubes
	Camera AB
	11 GM
	392 Flash Tubes
	3 G.M.
	Magnet Pole Pieces
	392 Flash Tubes
	11 GM
	Camera CB
	944 Flash Tubes
	25 G.M.
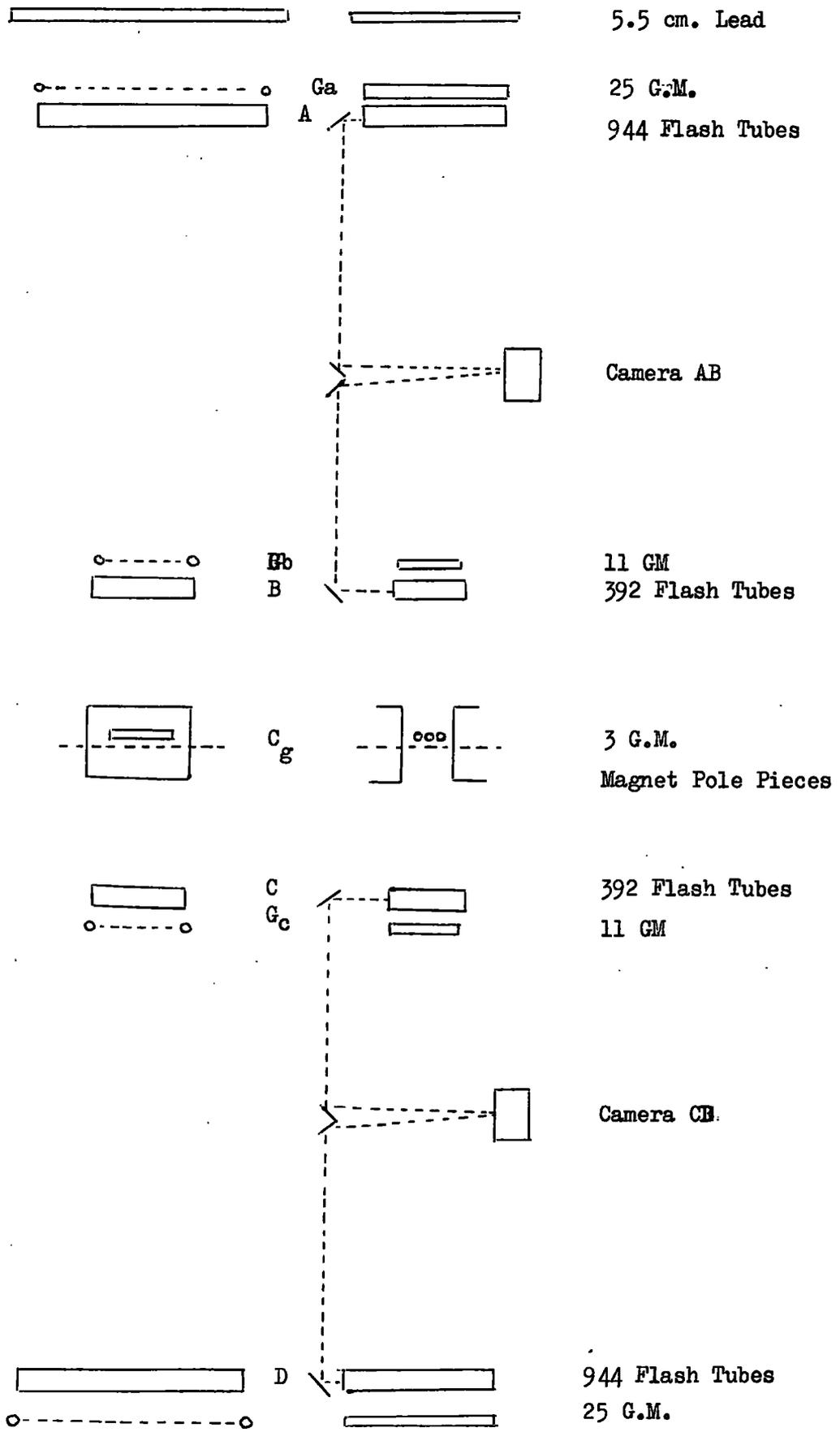
Fig. 4.   The Durham Spectrograph.

0 CM 50

The calculation of the deflection, Δ, is performed electronically with the aid of an analogue device, the momentum analyser. In each tray, when a geiger counter is discharged it will send a pulse to the analyser, the height of this pulse being linearly dependent on the position of the geiger counter in the tray. If the pulse from tray A has a height a and heights are similarly denoted for B, C, D, the analyser performs the calculation

$$\Delta_{MA} = \frac{(a-b)-(c-d)}{2}$$

Provided the condition of five-fold coincidence is satisfied, and only one pulse is received from each tray (so no knock-on particles are accepted), the resultant Δ_{MA} is shown as a deflection against a calibrated scale on an oscilloscope screen. This process is shown diagrammatically in Fig. 5.

Because of the size of the geiger counters, (diameter - 3.6 cm), the momentum spread for a given value of Δ_{MA} is quite large and increases as Δ_{MA} decreases. Thus a particle having $\Delta_{MA} = 0$ and hence, theoretically, of infinite momentum may, even at the highest magnetic field possible, have a momentum as low as 7 GeV/c.

The value $\Delta_{MA}/1.9$ is an integer and is termed the 'category number' of the particle. The factor of 1.9 arises from the separation between centres of the adjacent counters in the spectrograph.

Then category n has a nominal deflection of 1.9 n cm.

The deflection distribution for any category is shown in Fig. 6.

If the instrument is to be used to measure a momentum spectrum of the cosmic rays incident upon it account must be taken not only of the category acceptance function but also that for the spectrograph as a whole. The acceptance value for a given momentum, to the spectrograph, is a function of the aperture width G and the angle θ available for that momentum (see Fig. 8). The complete function is shown in Fig. 7 which shows three particles with the same momenta.

If we are to determine the mean momentum of a group of particles with the same category number we must know the differential momentum spectrum for each category and hence for the instrument as a whole. In the present experiment knowledge of these distributions is essential in order that we may assign the most probable ionisation
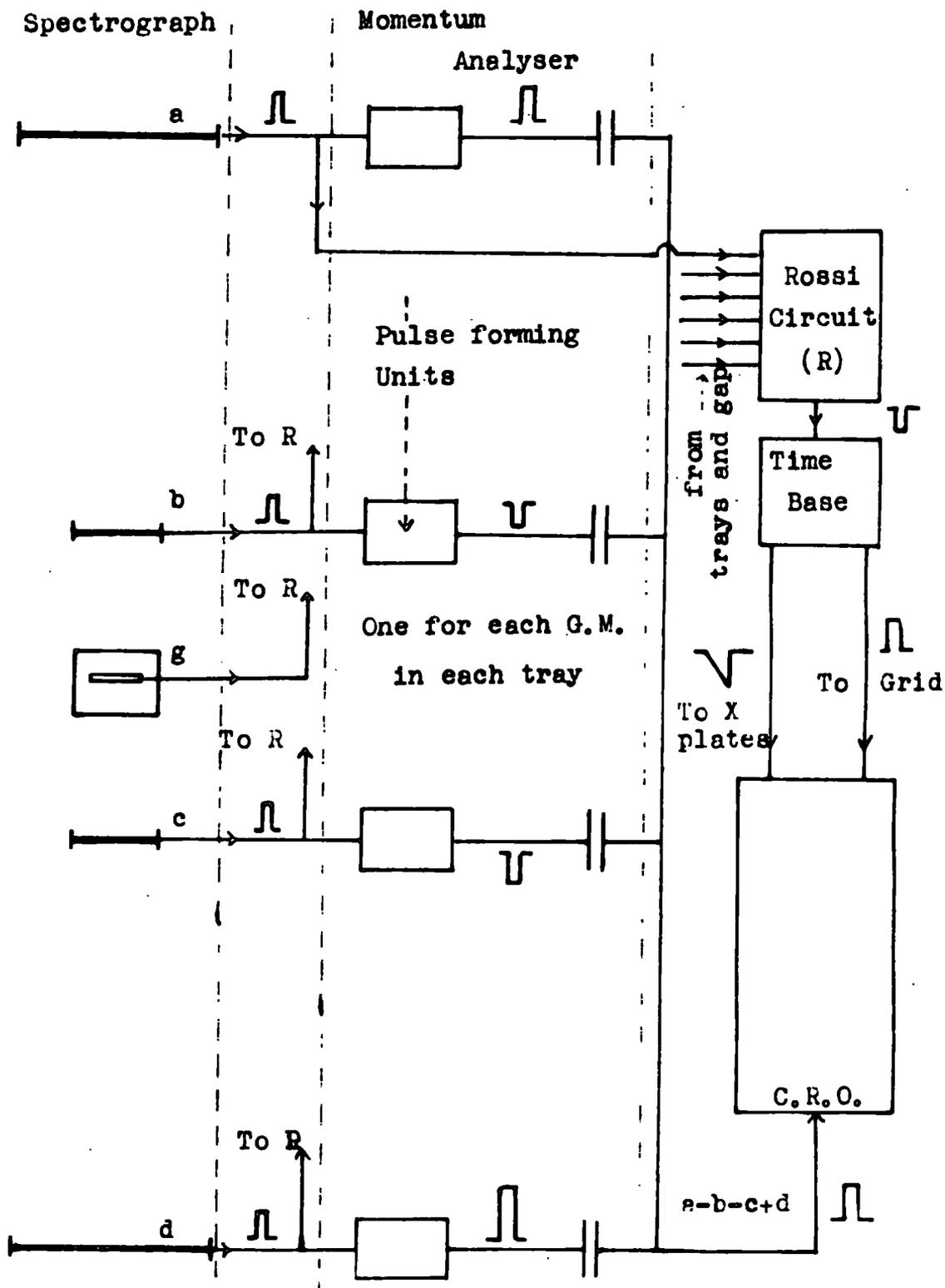
Fig. 5. Momentum Analyser (Diagrammatic)

Fig. 6 . The Category Acceptance Function.

(Area normalised to unity).

$\pm \Delta$ units of 0.2 cm.

Fig. 7 . The Spectrograph Acceptance Function.

Δ cm.
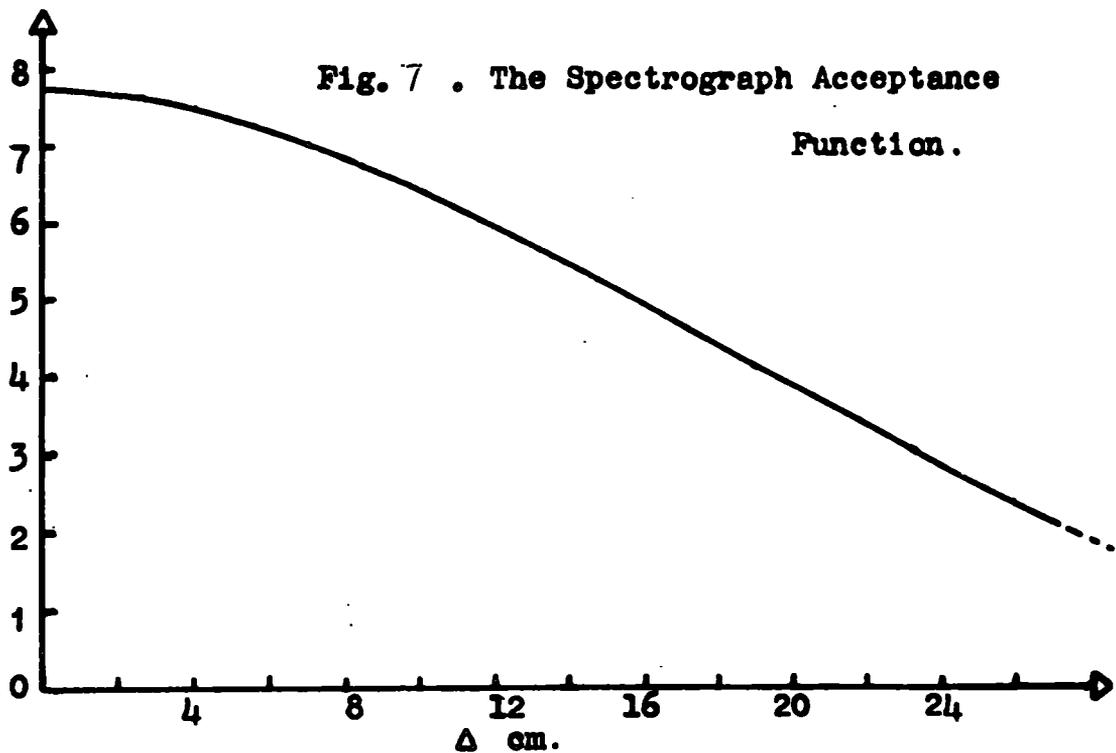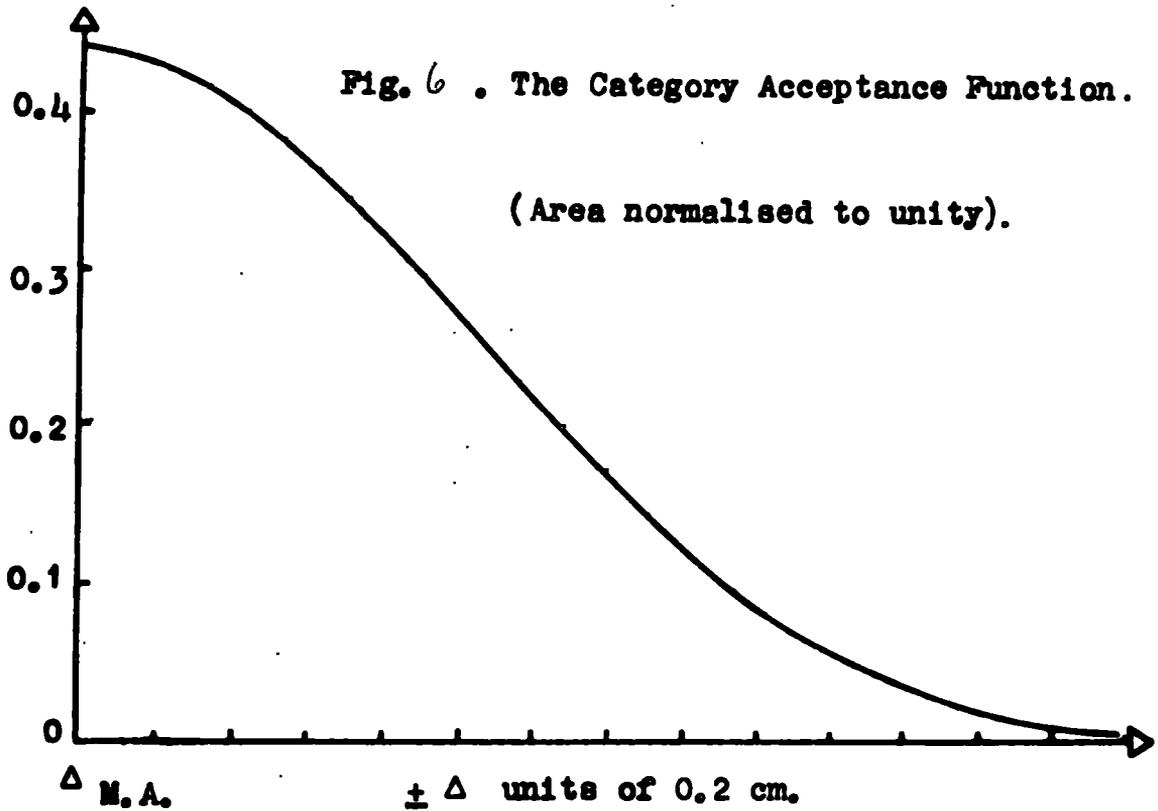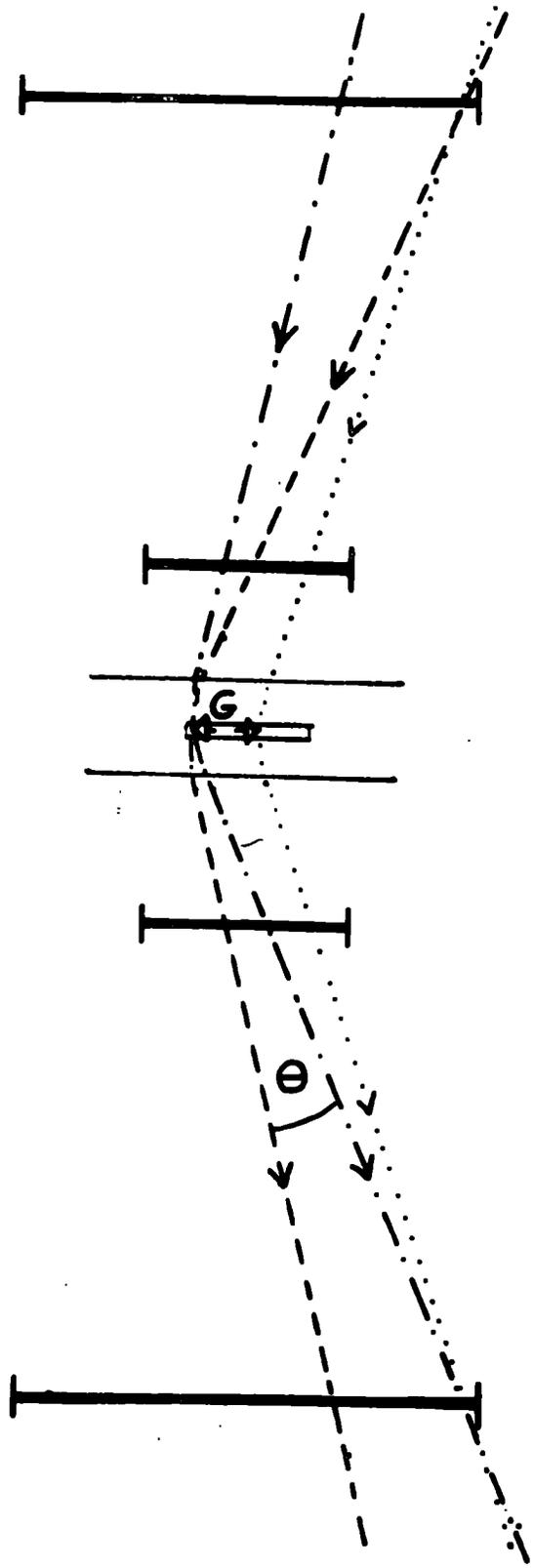
Fig. 8 . Spectrograph Acceptance (see text)

loss for a category to the appropriate mean momentum.

2.2 <u>Measurement of the ground level differential momentum spectrum of cosmic ray μ-mesons</u>

Experimentally, the total number of particles in each category is found, taking into account both positive and negative particles and both directions of magnetic field.

A trial spectrum is then selected, which should be as close to the correct result as possible. Originally at Durham a spectrum similar to those found by Owen and Wilson (1955) and Caro et al (1951) was adopted. This was converted into a differential deflection spectrum as followed:

Denoting momentum by p, and deflection by Δ. From the total number of particles

$$\int N(p)dp \;=\; \int N(\Delta)d\Delta$$

we may take $N(p)\delta p \;=\; N(\Delta)\delta\Delta$

i.e $N(\Delta) \;=\; N(p)\dfrac{dp}{d\Delta}$

but $p \;=\; \dfrac{k}{\Delta}$

$\therefore \dfrac{dp}{d\Delta} \;=\; \dfrac{-k}{\Delta^2} \;=\; \dfrac{-p^2}{k}$

i.e. $N(\Delta)= \dfrac{N(p)k}{2} \;=\; \dfrac{-N(p)p^2}{k}$

The following procedure is then followed.

a) Convert the momentum spectrum to a deflection spectrum

b) Multiply the deflection spectrum by the spectrograph acceptance function

c) Multiply by the category acceptance function centred on the appropriate nominal deflection for that category.

This gives the individual category spectra. Some of these are shown in Fig. 9, although these refer not to a trial spectrum but to the true spectrum. $\left(\text{Figs. 9b .9c} \right)$

The areas of these category distributions are found and the relative numbers in these distributions are compared with the relative numbers measured experimentally.

A graph of $\dfrac{\text{experimental numbers}}{\text{trial numbers}}$ against category, suitably normalised, is plotted and, if the trial spectrum is correct the result should be a horizontal line. Otherwise the trial spectrum is multiplied by this function and the whole procedure repeated until agreement is obtained.

It was found that this procedure was only necessary for the lower categories in the region where the deflection spectrum is rapidly varying $(n \leqslant 2)$. For the higher categories it is sufficient to use the number of particles
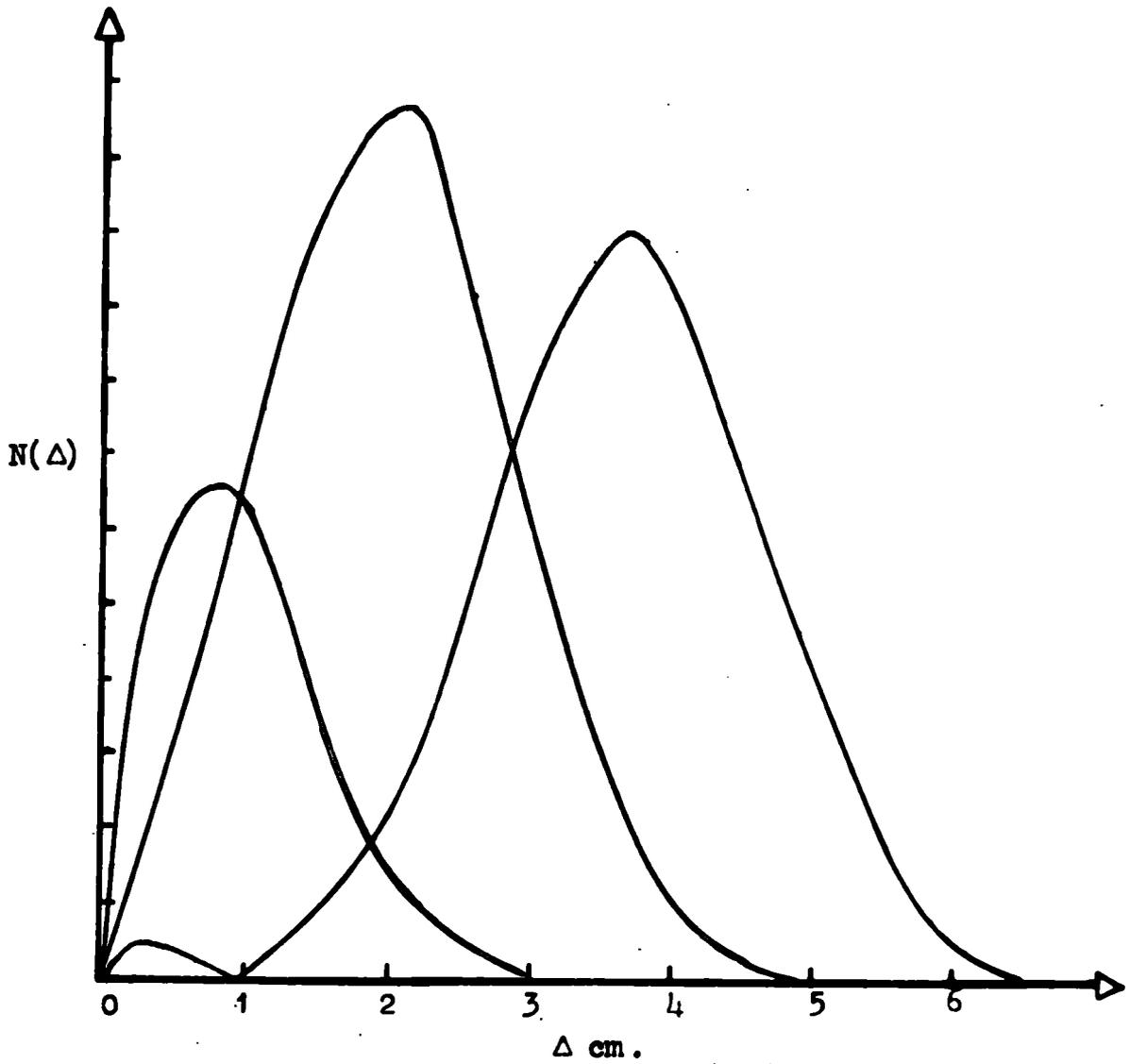
Fig. 9a . Differential Deflection Spectra for

Individual Categories.

(Categories 0, 1, 2)
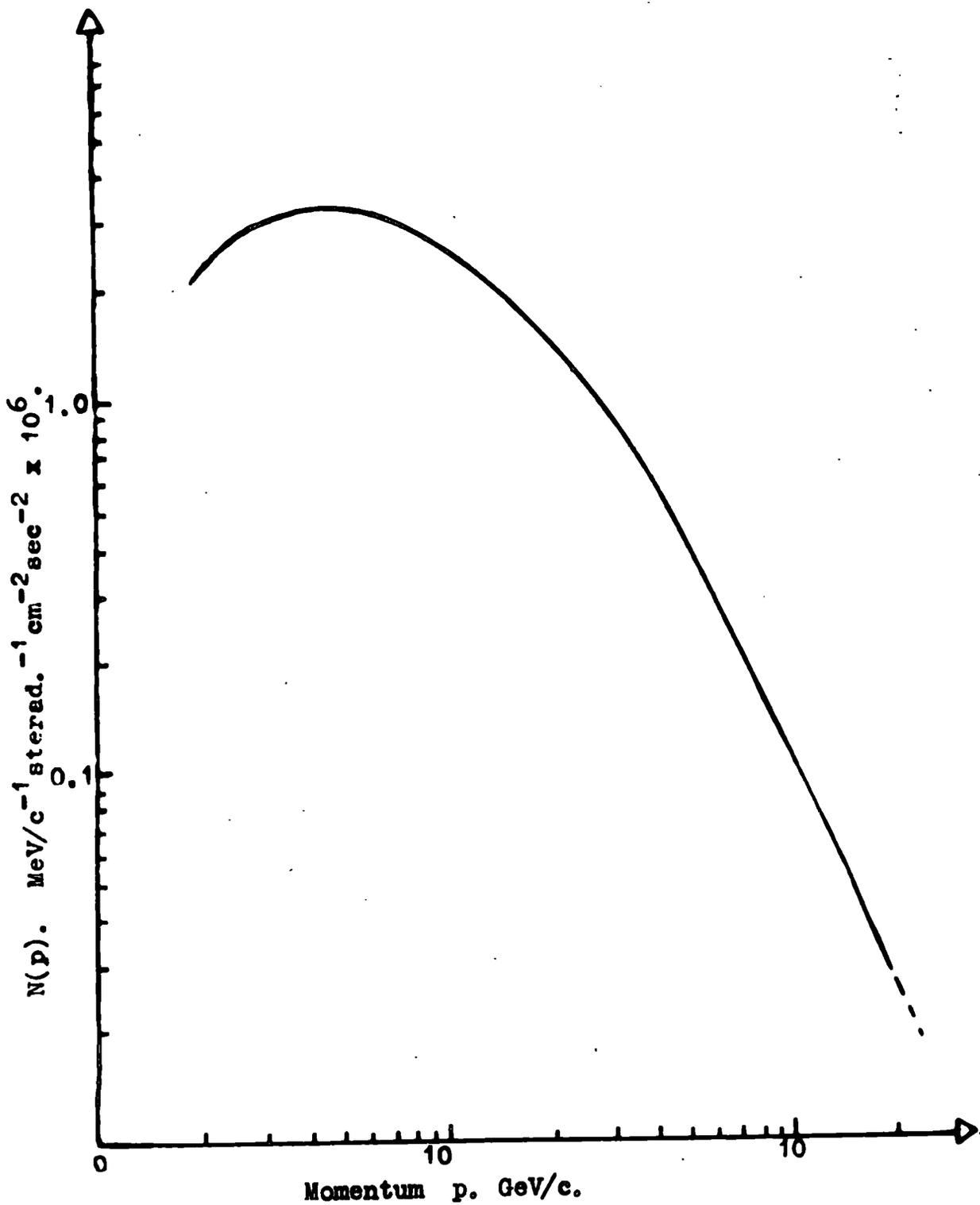
Fig. 9b . Spectrum of cosmic rays μ-mesons incident
on the Durham Spectrograph.
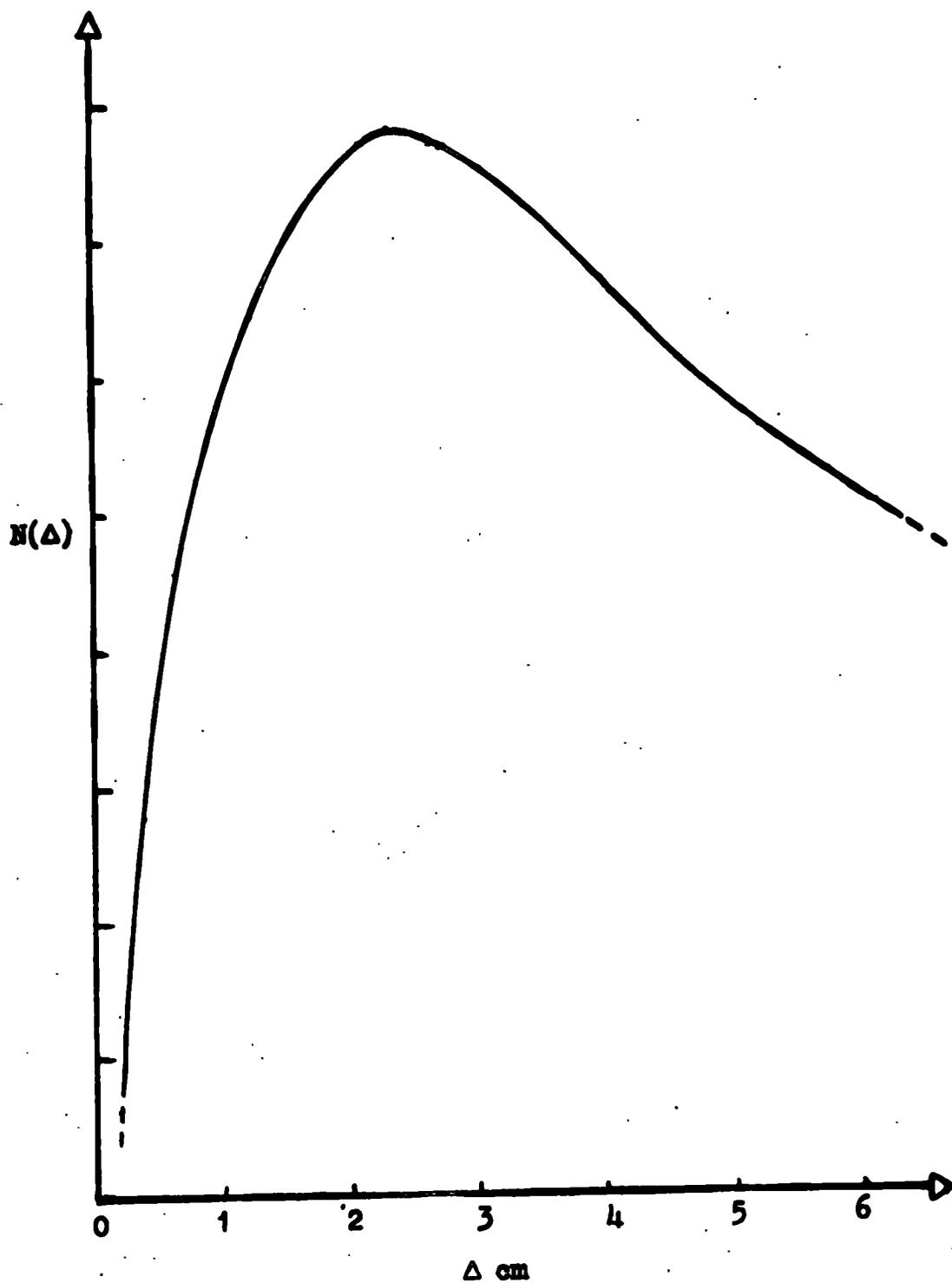
Fig. 9_c . Differential Deflection Spectrum of μ Mesons
for k = 17.42 .

found in a category as the ordinate of the <u>observed</u> deflection curve at the nominal deflection of the category. These ordinates are then divided by the spectrograph acceptance function to give the incident deflection spectrum.

When the geiger counters alone are used the maximum detectable momentum (m.d.m.) is about 25 GeV/c (the m.d.m. is defined as the most probable value of momentum for category zero).

The m.d.m. may be extended by more precise location of the trajectory at the four levels A, B, C, D. This has been made possible by using banks of neon flash tubes (Ashton et al, 1960). The first analysis using the flash tubes yields an m.d.m. of 150 GeV/c and a more careful examination using a track simulator technique gives an m.d.m. of 1000 ± 200 GeV/c.

2.3 The Momentum Selector

When the flash-tubes are being used, almost invariably only high energy events with momenta > 30 GeV. are of interest. To save analysis and recording film, there is an electronic 'momentum selector' which causes the high voltage pulse to be applied to the tubes only when a category 0 particle is registered by the momentum

analyser. In practice about 7% of category 1 particles are also accepted.

2.4 Results obtained for the Spectrum

The spectrum has been extended to the region of very high momentum with the use of flash tubes and the shape of the spectrum fairly well established. The statistical accuracy in the region of overlap with the counter results is not very high and the flash tube results have been normalised on to the counter spectrum by the method described earlier in §2.2.

2.5 Use of the Spectrograph as a Particle Selector.

The spectrograph may be used to select and identify the momenta of high energy cosmic rays. The overall rate of acceptance of particles when the magnet is operating on high field is about 170/hr.

In the experiments on ionization loss to be described the ionization detectors - proportional counters - were placed in position as shown in Fig. 10. In this case there is the additional coincidence requirement of the geiger-counter telescope associated with the proportional counters and the rate is reduced to about 50/hr. This position for the proportional counters was adopted as being the most convenient, both from the point of experimental
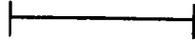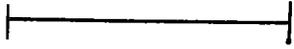
Tray A.
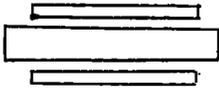
Proportional Counters
and Geigertelescopes
Tray B.

Gap Counters
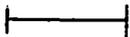
Tray C

0   50 cm
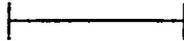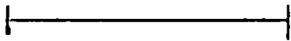
Tray D

Fig. 10. The Spectrograph with Proportional Counters.

procedure concerned with the counters, and the need to leave the spectrograph unobstructed while the present experiment was not running. A considerable improvement in rate would result if the proportional counters and telescope were to replace the gap counters both in position and function.

It is not certain that the proportional counters would work satisfactorily in this position, however, although Alikhanov et al (1956) have reported experiments in which proportional counters were operated in a magnet gap.

For the experiments to be described the flash-tubes were not operated, momentum measurements being afforded by the momentum analyser, which uses the geiger counters only.

It is intended that the studies should be extended to higher momenta by the use of the flash-tubes in association with the momentum selector, when the rates will be (for counters in the magnet gap):

<div align="center">

3/hr   above   30 GeV/c.

0.5/hr   above 100 GeV/c.

0.04/hr   above 500 GeV/c.

</div>

CHAPTER 3

PROPORTIONAL COUNTERS

3.1 Basic Principles of the Electrical Counters.

The proportional counter belongs to a large family of radiation detectors, which depend for their operation on the production of ionisation in a gas between two electrodes maintained at different potentials. The ions of one, or both, signs, depending on the type of detector, are collected and produce a pulse at the electrodes. This pulse may be, if necessary, amplified, and will serve to indicate the presence of an ionizing mechanism within the gas.

If the voltage across the electrodes is not very high, some of the ions will be lost primarily by recombination. This is the mode of operation of the ionization chamber, where, unless the original ionization is very heavy, the device must be used as a collection chamber, otherwise the pulse will be too small to be amplified.

However, as the applied voltage is increased, a stage may be reached at which the electrons will be sufficiently accelerated between collisions that they cause secondary ions to be produced and the number reaching the electrodes will be greater than the number

originally produced. This effective amplification within the device itself greatly increases the range and the usefulness of this type of detector.

It is easily shown that if the electrodes are plane the size of the pulse is dependent on the position of the original ionization in the chamber and, if due to the passage of a charged particle, on the orientation of the track. Also, if internal multiplication is used for amplification then this too will depend on the location of the original ionization.

To avoid this difficulty it is customary with pro-portional counters and geiger counters, the classes which do utilise gas multiplication, to adopt co-axial electrodes, the inner one being in the form of a fine wire.

Then, if the electrodes are cylindrical, the inner one having a radius a, and the outer a radius b, the voltage at any radius r, V_r, is given by

$$V_r = V \frac{\ln \frac{r}{b}}{\ln \frac{r}{a}}$$

Where V is the applied voltage and b > r > a.

If the ratio b:a is very large then a considerable fraction of the total voltage drop will occur very close to the central electrode.

Now let us define V_{crit} as that voltage for which multiplication is likely to begin. Then if the applied voltage V is so adjusted that r_{crit} is a few times a' we may obtain constant amplification for any pulse, regardless of the original position of the ionization within the chamber, excepting the very small proportion of it that may occur at $<r_{crit}$.

This will be seen more clearly in the next section when the question of gas multiplication and pulse formation will be examined more closely.

We may now, however, define the limits of the various types of counter we have been discussing, by means of the graph shown in Fig. 11, which shows the variation of pulse height with applied voltage under the condition of constant original ionization within a cylindrical counter of the form already described. The relation for two values of ionization are shown.

Region 1: No gas multiplication is occurring and this is the condition for an ionization chamber.

Region 2: Here there is moderate multiplication, which increases with voltage and since here the resultant pulse height is very closely proportional to the amount of ionization originally produced, is the proportional counter region.

Region 3: Here secondary ionization is implemented
by photons and their resultant photoelectrons so that
the presence of any ionization will initiate multiplica-
tion along the whole length of the inner electrode, with
the result that all pulses produced in this region are
of the same height. This is how geiger counters are oper-
ated and here the pulse may be of the order of volts, so
that an amplifier is not always necessary.

3.2 Gas multiplication in the proportional counter

We will now confine attention to Region 2, where the
gas multiplication is moderate. The ions are generally
separated quickly enough in a proportional counter to
make recombination between these ions an unimportant
factor. Care is taken to avoid the loss of electrons by
the production of negative ions i.e. the attachment of
electrons to neutral molecules. This is achieved by
strenuously excluding electronegative gases (e.g. O_2,
H_2O). Thus the electrons, with their much greater mobil-
ity, are drawn towards the anode which is the central
wire.

Let us define λ as their mean free path between
collisions. Then at r_{crit} the field E is such that

$$E \lambda = V_i$$

——————— :- from Counter

— — — — :- from Counter and
           electronics

Several m.s.

Full Pulse
Height

<1μs>

< several >
    μ s

Time

Fig. 12 . Proportional Counter Pulses.

Pulse

Height

1

2

3
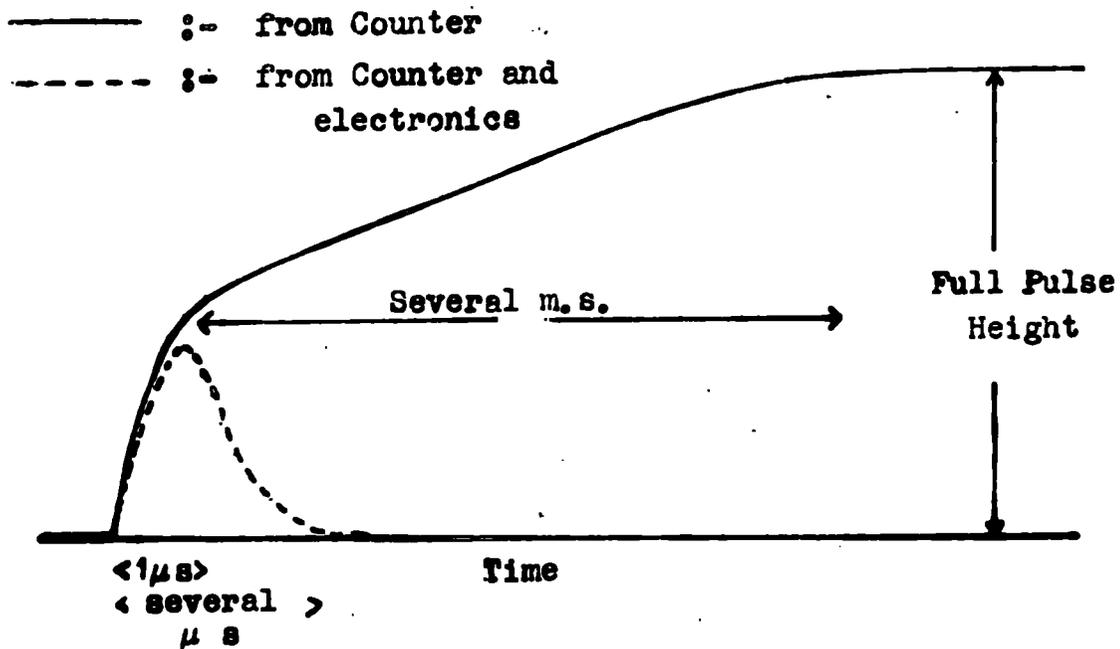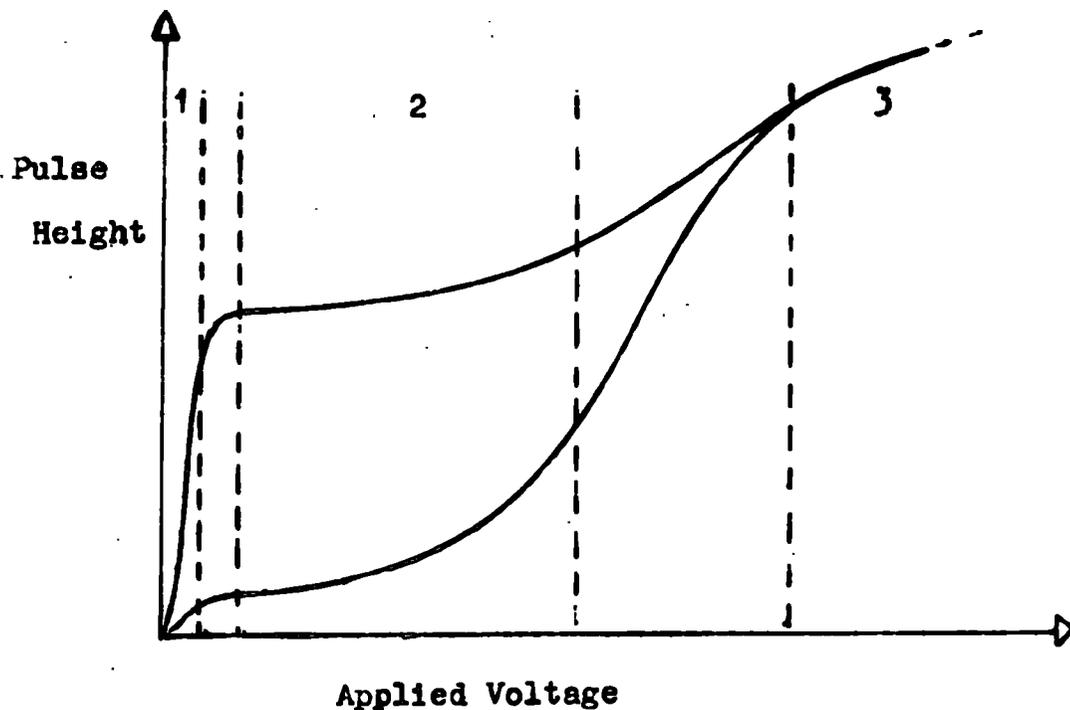
Applied Voltage

Fig. 11 . Variation of Pulse Height with Applied Voltage.
          Counters with Concentric Electrodes.

where V_i is a voltage which we may take to a good
approximation as the mean ionization potential of the
gas in the counter. A collision may then create a
secondary ion pair and the electron of this together
with the original electron can go on to produce other
secondary ionizing collisions.

If the primary electron has m such collisions it
is easily shown that 2^m electrons will result. Thus

$$A = 2^m$$

where A is the Gas Multiplication Factor.

For proportional counters this is the major method
of multiplication, but for $A > 10^4$ the contributions
from photoelectrons ejected from the cathode become
important. If γ is the probability that one photoelec-
tron-ion pair is produced in an avalanche then the gain
become $\dfrac{A}{1 - \gamma A}$.

Thus if $\gamma A = 1$ the gain is theoretically infinite
and in fact the 'geiger' region has been reached. But
for values of γ less than $\frac{1}{A}$ a finite gain still results;
and a proportional response may still be obtained. It
is obviously advisable, though, to operate at moderate
values of A if an accurately proportional operation is

required and this condition is emphasised by the fact
that at large values of A avalanches may overlap to the
extent that mutual interaction will reduce the pulse
height produced.

Curran & Craggs have produced a theoretical treat-
ment of the dependence of multiplication upon the
variables of the counter under the conditions of moderate
A, low enough to avoid photoelectron effects, and high
enough to avoid recombination, and the theory appears to
be in quite good agreement with experiment. We will only
concern ourselves with the dependence on applied voltage, V_A,
here, which takes the form

$$A = \exp\left\{ \text{Const.} \, V_A^{\frac{1}{2}} \left[\frac{V_A^{\frac{1}{2}}}{\text{Const.}} - 1 \right] \right\}$$

Showing that the logarithm of amplification should
increase linearly with the applied voltage.

3.3 Pulse Formation

The electrons in a counter of normal dimensions
(of a few cms.) will be collected in about 1 μs. But
the +ve ions, the majority of which, indeed virtually all
if A≫1, are concentrated close to the wire, have a much
lower mobility and these control the pulse, as they move
out towards the cathode, and control its length.

It can be shown (Wilkinson 1950) that the signal
at the wire S(t) after a time t from the ionization
event is given by

$$S(t) = \frac{-e}{2\,C\ln\left(\frac{b}{a}\right)}\,\ln\left\{1 + \left(\frac{b^2}{a^2} - 1\right)\frac{t}{T}\right\}$$

where T = the collection time for positive ions and C
is the capacity of the counter system.

The form of this is shown in Fig. 1a. We see that
it consists of a fast initial rise, followed by a pro-
longed increase to the maximum S(T). This may be
qualitatively explained by the fast initial drift of
the +ve ions in the high field region followed by a
slower approach to the cathode. More precisely we see
that at $t \overset{\sim}{=} \frac{a}{b}$ T $S = \frac{q}{2C}$

but $\frac{a}{b} \overset{\sim}{=} 10^{-3}$

and $T \overset{\sim}{=} 1$ ms,

thus the signal half height is reached in approximately
1 μs.

If we are able to neglect the effect of different
collection times for the electrons, it is possible to
reject the slow development region without affecting the
proportionality of the signals (i.e. we may use an
amplifier with a short differentiating time on the input

such that the pulse is reduced to the form shown in Fig. 14). Thus, instead of a pulse of several milliseconds duration, we are able to 'clip' it to a few microseconds. This increases the sensitivity of the counter and enables it to be used in coincidence systems, and at faster counting rates, than would otherwise be possible. Generally, for most counters, an integrating time constant which is not greater than the differentiating time constant, and is of the order 10^{-5} - 10^{-6} sec proves suitable.

It is convenient here to consider briefly the benefits of gas amplification in overcoming noise in the amplifiers and associated electronics.

In the type of experiment considered here we are dealing with cases where the original number of ion pairs may not be greater than about 25. The noise level of a good amplifier will be 3.10^{-5} volt. If we take the capacity of the counter electrodes to be 10 pf this is quivalent to the collection of approximately 2000 electrons by the wire. Thus if we are to have a signal to noise ratio 10:1 the original number of electrons in the counter must be increased by a factor 1000. This is done by the multiplication process.

3.4 Spurious Effects in Proportional Counters and Gas Filling

It is true to say that all the spurious effects present in a Geiger counter will also be present to some degree in a proportional counter.

These are

a) ejection of photoelectrons from the cathode by the positive ions

b) metastable atoms, which give off photons. These may produce electrons

c) Paetow effect; delayed ejection of electrons

d) Negative ions formed by the attachment of electrons to electronegative impurities. These electrons may be stripped off in the high field region.

However the requirements for correct operation in proportional counters are very much less severe. Whereas in a geiger counter a single photoelectron will initiate a discharge, in a proportional counter up to a limit already defined, the photoelectrons will not have any serious effect.

Care is taken, however, to avoid the loss of electrons by the production of negative ions. This is achieved by strenuously excluding electronegative gases.

Otherwise very few gases are not suitable for proportional counter operation in some proportion even water vapour being tolerable up to 1 cm Hg pressure.

The light inert gases have the advantage that they require a lower potential for a given counter, gas pressure and multiplication than most other gases, but the tendency to form metastable states makes it advisable to add a proportion of a polyatomic organic vapour, these usually having a high cross-section for absorption of photons.

Organic vapours may be used by themselves in proportional counters and in many cases it may be preferable to do so. Methane and propane have been widely used.

3.5 Defects due to Counter Geometry

a) Irregularity in Electrodes

If the central electrode has a varying radius or protuberances on it, the gas amplification will be greatly affected due to the sharp variation of voltage in this region. Irregularities in the cathode are not so serious. Also, Rossi and Staub (1950), have shown that the extreme fractional difference of the field $\frac{dE}{E}$ due to the wire being displaced a distance 'd' from the central axis is given by

$$\frac{dE}{E} = \frac{4a \cdot d}{b^2}$$ where a and b are the anode and

cathode radii and generally since $E = \frac{V_O}{r \ln \frac{b}{a}}$ this effect is only serious
at high pressures (Appendix 1).

b) End Effects

The junction of the wire with the end of the proportional counter will distort the field in this region and lead to variations in amplification. The extent of this variation, and measures which may be taken to overcome it, are described by Curran (1959) where other defects are also described.

3.6 Counters used in the Present Experiment

a) Special Requirements of Geometry

Since we wish to measure the rate of ionization loss of a charged particle we obviously cannot use a cylindrical counter since we would then be unable to define the track length. A rectangular counter has been chosen so that the beam of particles can have a constant track length by crossing the counter perpendicularly to the walls. The anode is a cylindrical wire. A graphical solution of the field has been made for this type of counter and is shown in Appendix I

We see that the field is radial up to a distance comparable with the cathode dimensions and much of the discussion of cylindrical counter theory will still apply sufficiently for our purpose.

b) Construction of the Proportional Counters.

The counters used in this experiment were made by D.G. Jones of this department. They are basically lengths of rectangular copper wave guide with a cross-section $\overset{10.92 \times}{5.45 cm}$ a length of $76cm$, and a thickness of metal of $0.2cm$ The anode is of $0.01cm$ diameter tungsten wire sealed into glass insulators at the junctions with the ends of the counter. There are two mica windows in the top of the counter for calibration by X-ray sources. A counter is shown in Fig. 13.

c) Counter filling

The counters are filled with neon to 40.5 cm Hg pressure and have an additional 2.9 cm Hg of methane as a stabilising agent.

d) Operating Conditions

The counters are operated at a potential difference of about 1000 volts when the loss of 10 keV energy in the counter will cause a pulse 0.1mv to be sent to the head amplifier. The E.H.T. is provided by a stabilized pack giving a voltage steady within 0.1%.

Fig. 13   Proportional Counter
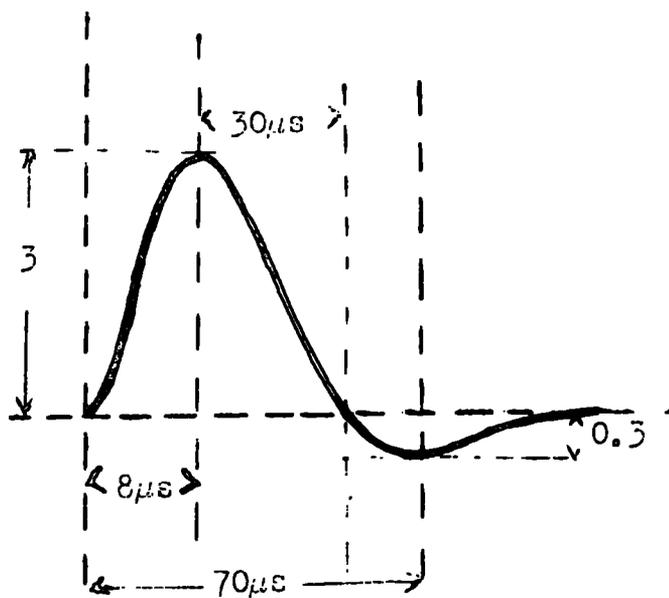
Fig. 14   Typical Pulse (after amplification)

The head- and main-amplifiers are commercial units (Dynatron) and are operated with the integrating time constant equal to the differentiating time constant in the main amplifier, both having the value of 8μsec.

Pulses similar to those shown in Fig. 14 are produced.

3.7 The Geiger Telescope

The particle trajectory through the counter is defined by requiring that it pass through a geiger telescope. This consists of two geiger counters, of similar length to the proportional counter, arranged one above and one below that counter so that their axes lie in the same plane as that of the proportional counter. A section through the three counters is shown at the top of Fig. 16.

CHAPTER 4

THE ELECTRONIC CIRCUITS

4.1 General Arrangement

A block diagram of the apparatus used in the proportional counter experiment is shown in Fig. 15. The pulses from the geiger telescope are taken to a two-fold coincidence unit, which, if coincidence occurs, will send on a pulse to an additional Channel of the main Rossi coincidence circuit. If a six fold coincidence is registered between ABCD, this additional channel, and the gap counters, the momentum analyser unit sends a pulse to the category recording oscilloscope and also sends a pulse to the main triggering unit. This then triggers an oscilloscope which has the proportional counter pulse from the amplifiers fed on to the Y-plates via a delay line. A delayed trigger pulse also provides a base line from which to measure the height of the counter pulse. Also triggered by this circuit is a neon bulb hodoscope actuated by the two-fold coincidence unit which indicates, by the counter oscilloscope screen, which proportional counter the particle has passed through. At the same time the cycling system is set in motion, illuminating clocks and moving on cameras.
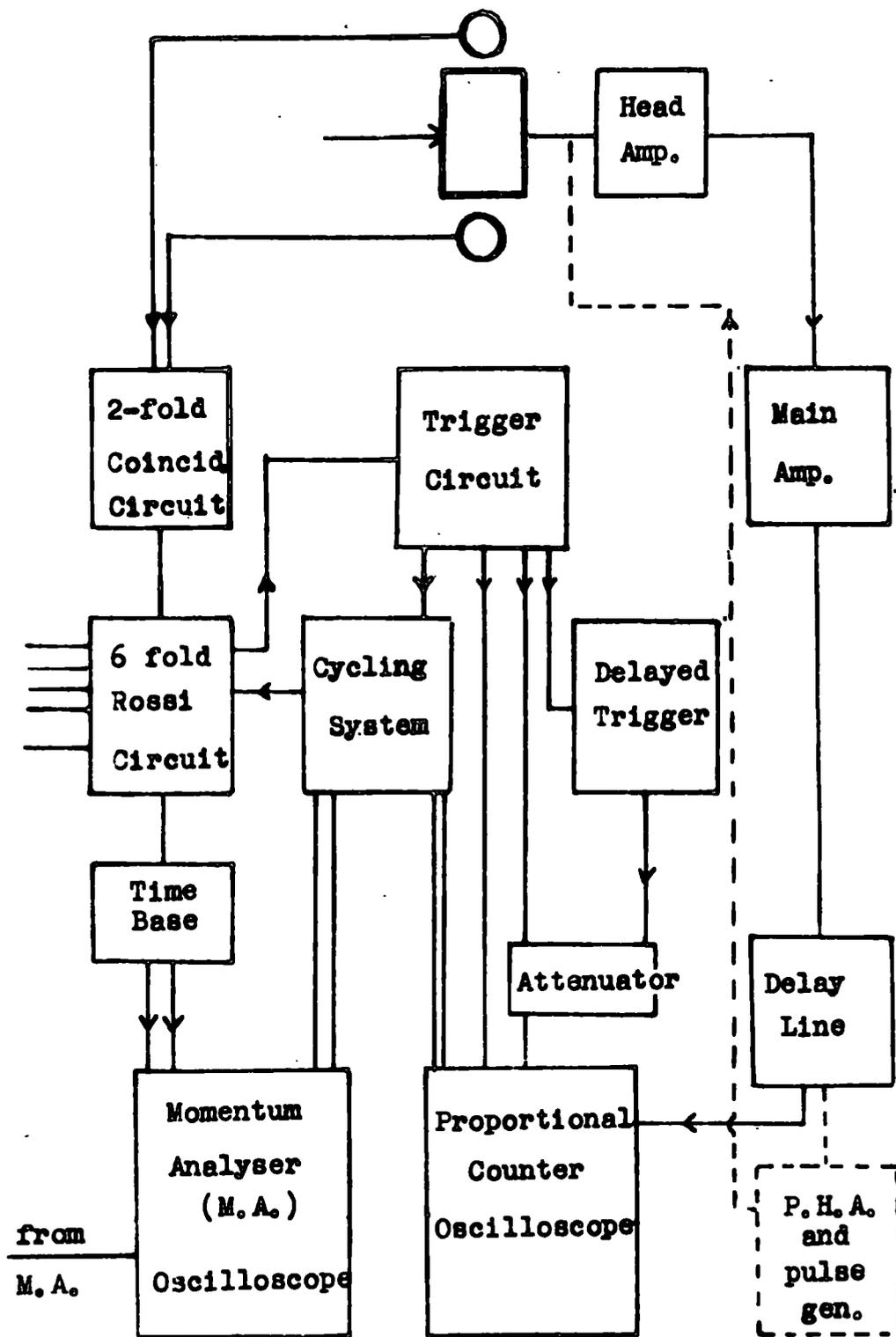
Fig. 15 . Proportional Counter Experiment: Diagrammatic.

4.2   The Proportional Counters

In the present experiment two proportional counters were used side by side using the same E.H.T. voltage, a negative voltage being fed to the cathode by means of a metal 'saddle' fitting across the counters at their ends.   There was no other conducting connection between the counters.   These rested on Perspex strips fixed to the bottom of a metal box completely enclosing the counters (Fig. 18).   The geiger telescope had the top layer inside the lid of the box, which was itself attached to a trolley which could be wheeled into the particle beam.   Also on the trolley were the geiger quenching units and the proportional counter head amplifier.

4.3   The cycling System

This is an electronically actuated relay system which illuminates the clocks above the oscilloscope faces, moves on the film in the cameras by the required amount, and paralyses the main Rossi coincidence circuit throughout the cycling period.   The clocks enabled the two films to be correlated.

4.4   The Pulse Height Analyser and Pulse Generator

The pulse height analyser has 100 or 150 channels and incorporates a pulse generator (Marshall's of

Cambridge). The channel width is correspondingly ½/½ volt and by using a bias it will accept pulses of up to 100v. The input gain may be increased to two or five times. The analyser was used in the calibration of the analyser or for calibrating the proportional counter amplifiers and the oscilloscope, which was run from a stabilised main supply.

4.5 Calibration of the Proportional Counters

The calibration was effected by using an X-Ray source which ejects photoelectrons in the gas having a single energy, all of which will be lost in the counter gas. Sources were chosen with energies in the same region as those lost by cosmic ray μ-mesons passing through the counter. Two sources were used to check that the amplification was linear, though these strictly will only show whether the amplification is consistent with linearity. Details of these sources are given in Appendix II.

If it is assumed that the energy required per ion pair is the same for electrons as for μ-mesons, it is possible to give an absolute result for the ionization loss of μ-mesons in a gas, but this assumption is not really justified. The primary purpose of the cali-

bration was to ensure that there was no appreciable
drift in the total amplification provided by the
counter and the associated amplifiers.

The sources were also used, in determining the
variation of gas multiplication with applied voltage,
to study statistical variations of pulse height and to
show that stray magnetic fields had no effect on the
pulse height.

The calibration of the counters was normally carried
out at the beginning, middle, and end of a twenty-four
hour run.

4.6   Recording of Results

The amplified proportional counter pulse and the
category number of the effective particle are displayed
on different oscilloscopes, and hence will be recorded
on two different films. Despite marking the film at
the beginning and end by illuminating the C.R.O. face,
it was necessary to have some means of correlating events
on the two films, and thus on each record was included
the time indicated by a watch, these being illuminated
for 1sec after the camera has been moved on. Both
cameras were operated with continuously open shutters.
At·each calibration of the proportional counters, test
frames were taken on the momentum selector film calibra-

ting the scale of this screen and checking that the
operation of the selector was satisfactory.

CHAPTER 5

The Average Ionization Loss of a Fast Charged Particle

The theory concerning the average energy loss of a fast charged particle is well established. Differences between individual treatments of this theory are small, and exist mainly in the transition region between the 'log rise' and the plateau. The simple classical theory of ionization loss was given first by Bohr (1915). Developments of this theory and later quantum mechanical versions all yield the same general results for the variation of ionization loss with energy. These were outlined in Chapter 1.

5.1. The Bohr Theory

In Fig. 17 is shown the charged particle (charge ze) and its path. The theory considers the electric intensity E leaving a cylinder which has as its axis the path of the particle, and a radius b. This field acts on the electrons of the medium for a short time, providing an impulse which causes excitation or ionization.
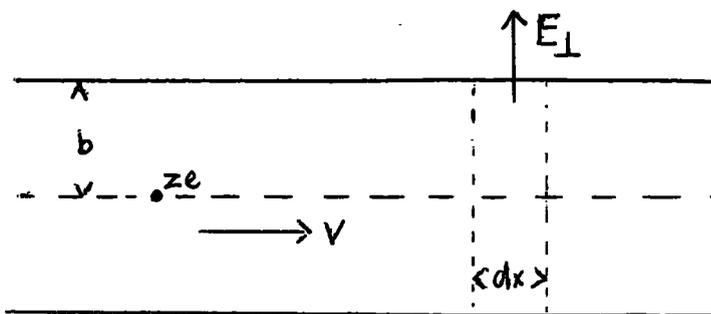
Fig. 17.

From Gauss' Law we have $\int E \cdot dA = 4\pi ze$.

i.e. $\int_0^b E_\perp 2\,b\,dx = 4\pi ze$.

$\therefore \int E_\perp dx = \dfrac{2ze}{b}$.　　　　　　　　(1)

If we consider the particle to be fixed and consider a moving section of the cylinder

Then $\displaystyle\int_{-\infty}^{+\infty} E_\perp(t)\,dt = \int_{-\infty}^{+\infty} E_\perp(x)\dfrac{dx}{v}$　　　　(2)

where v = velocity of the particle

　　　t = time.

$\therefore$ From (1) + (2)

$e\displaystyle\int_{-\infty}^{+\infty} E_\perp dt = \dfrac{2ze^2}{bv}$

But this is the total impulse acting on the electron of the medium due to the passage of the particle.

i.e. momentum gained $p = \dfrac{2ze^2}{bv}$

$\therefore$ energy gained $\dfrac{p^2}{2m} = \dfrac{2z^2e^4}{mb^2v^2}$　　　　　(3)

The number of electrons in the element of path dx between b and b+db is given by

$$2\pi \, b\,db \; NZ \; dx. \qquad\qquad (4)$$

where N = no. of atoms/unit vol.

Z = atomic number of the medium.

Thus from (3) and (4)

The energy loss from the charged particle

$$-dE = \frac{p^2}{2m}$$

$$\therefore \; -\frac{dE}{dx} = \frac{4\pi 3^2 e^4 NZ}{mv^2} \int_{b_{min}}^{b_{max}} \frac{db}{b}$$

$$= \frac{4\pi 3^2 e^4 NZ}{mv^2} \ln \frac{b_{max}}{b_{min}}$$

When the limits are considered, including the relativistic case.

$$-\frac{dE}{dx} = \frac{4 \; 3^2 e^4 NZ}{mv^2} \ln \frac{1.123}{2 \; ze^2 \bar{\nu}} \frac{v^3}{1-\frac{v^2}{c^2}}$$

where c = velocity of light

$\bar{\nu}$ = weighted mean of the vibration frequencies of the electrons in the atom.

5.2. The Bethe-Bloch Theory

More refined classical treatments have been made by Bethe and Bloch (1933).

In Bethe's theory, the collisions experienced by the fast particle are divided into two classes.

a) Distant collisions: An electron with energy less

than η is ejected.

b) Close collisions : An electron with energy

greater than η is ejected.

If η is small then the primary particle may be treated as a point charge.

If η is sufficiently large the atomic electrons may be regarded as free for close collisions. It is found that if $10^4 < \eta < 10^5$ eV then both of these conditions may be satisfied.

In a collision the electron may receive energy t where $I < t < T$.

I is the effective ionization potential weighted according to the probability of ionization and excitation in the atomic system and must, at present, be determined experimentally.

T is the maximum transferable energy to the electron.

The Value of I

Measurements of I by Bakker and Segre (1951) and Marker and Segre (1951) show I/Z increases from 9.3 eV to 15 eV as Z decreases.

In 1933 Bloch suggested as a good approximation

$$I(Z) = I_0 Z = 13.5 Z$$

This is acceptable since only ln I occurs in the

energy loss expression (q.v) and thus small variations in I will have little effect on the value of this expression.

Sternheimer (1956) however on studying the results of Caldwell (1955) prefers the relationship

$$I(Z) = 13.0Z.$$

The Value of The Maximum Transferable Energy

For $t \gg \eta$ the atomic electron may be regarded as a free particle.

Bhabha (1937) has shown that in the general case

$$t_{max} = T = \frac{E_o^2 - \mu^2 c^4}{\mu c^2 \left[\frac{\mu}{2m} + \frac{m}{2\mu} + \frac{E_o}{\mu c^2} \right]}$$

Where m = mass of the electron

μ = mass of the incident particle

E_o = Total energy of the incident particle.

In the case where $\frac{E_o}{\mu c^2} \ll \frac{\mu}{m}$ and $\mu \gg m$

$$T = \frac{2mc^2 \beta^2}{1 - \beta^2} \qquad (5)$$

We see that for μ-mesons ($m_\mu \tilde{=} 207\, m_e$) that the second condition is satisfied, and the first condition for meson energies $\ll 20$ GeV/c.

The second condition is not applicable to the range of energies we wish to cover and we see that, at 20 GeV/c, the true value of T is less than that given by the approximate equation by a factor of three. However as T also occurs within the logarithmic term, the approximate form will not introduce a large error.

Energy Loss in Distant Collisions $I \leq t \leq \eta$

This is given by Bethe (1930, 1932) as

$$-\frac{dE}{dx}_{coll} = \frac{2\pi NZr_o^2}{A} \frac{mc^2}{\beta^2} \left[\ln \frac{2mc^2 \beta^2}{(1-\beta^2) \cdot I(Z)^2} - \beta^2 \right]$$

where $r_o = \frac{e^2}{mc^2}$

and N is Avogadro's number.

Energy Loss in Close Collisions $\eta \leq t \leq T$.

In close collisions the electron is affected by the spin of the charged particle and this must be taken into account in the theory. This is given by Bhahba (1938) and Massey and Corben (1939) as

$$-\frac{dE}{dx}_{coll} = \frac{2\pi NZr_o^2}{A} \frac{mc^2}{\beta^2} \left[\ln \frac{I-\beta-\frac{1}{4}}{\eta} \cdot \left[\frac{T}{E+\mu c^2} \right] \right]$$

for a particle with spin $\frac{1}{2}$ and Kinetic Energy E. The last term is the contribution of the spin of the particle Total average energy loss.

Adding the contributions due to each type of collision we get

$$-\frac{dE}{dx}_{coll} = \frac{2\pi NZr_o^2}{A} \frac{mc^2}{\beta^2} \left[\ln \frac{2m\beta^2c^2T.}{(1-\beta^2)\,I(z)} -2\beta^2 + \frac{1}{4} \left[\frac{T}{E+\mu c^2} \right] \right]$$

and if we substitute for T from (5) this becomes

$$-\frac{dE}{dx}_{coll} = \frac{4\pi NZr_o}{A} \frac{mc^2}{\beta^2} \left[\ln\frac{2m\beta^2c^2}{I(2)} - \ln(1-\beta^2) - \beta^2 \right]$$

This is if we neglect the spin term which becomes small at high energies.

The Bethe-Bloch treatment gives a value for $\frac{dE}{dx}$ approximately twice that calculated using the simple classical method.

It shows an improvement in its treatment of collisions involving small transfers of energy. It recognises that the probability of this type of transfer occurring is governed by the energy levels of the electrons in the atom.

The formula derived is applicable to all charged particles except electrons. Here the two particles involved in a collision are indistinquishable. It is conventional to take as the surviving 'incident' electron that which has the greater energy after the collision. Thus in this case $T = \frac{1}{2}(E_o - mc^2)$. The expression for energy loss by close collisions must be modified, especially the terms involving spin effects.

The resultant total average energy loss for electrons was given by Möller (1932) as

$$-\frac{dE}{dx}_{coll} \text{ (electron)} = \frac{4}{A} NZr_0^2 \frac{mc^2}{\beta^2} \left[\ln \frac{2m\beta^2c^2}{I(Z)^2} - \frac{3}{4} \ln(1-\beta)^2 - \frac{1}{2} \ln 8 + \frac{1}{10} \right]$$

5.3. The Density Effect

The problem of ionization loss has so far been sim-
plified by treating each atom as isolated from its neigh-
bours, and thus ignoring any effect these might have on
the collision. But, as was first pointed out by ~~Sevann~~ Swann
(1938), the medium will be polarized by the field of the
particle and the polarization field will cancel out that
due to the particle at atoms not close to its path. We
would then expect that distant collisions would be affected
and that little difference would be made in the case of
close collisions.

Since, as we have already shown, the log rise is
partially due to the increased radius of action of the
particle's field, the polarization effect should be more
pronounced at higher energies.

This was first expressed quantitatively by Fermi
(1939, 1940), who considered only collisions sufficiently
distant that the medium was sensibly uniform and that the
electrons could be represented as classical oscillators,
with the further simplification of a single characteristic
frequency. The close collisions were accounted for by
interpolation between his treatment and Bethe's.

The theory was later extended by Halpern and Hall (1940, 1948) using a model having several characteristic frequencies. Other work has been done by Wick (1940, 1943), Schönberg, and especially by Sternheimer whose calculations are the most extensive.

His expressions for the density effect and its variation with pressure in the case of a gas are given in Appendix III.

5.4. <u>The Role of Cerenkov Radiation</u>

Cerenkov radiation, first investigated by Mallet in 1926, occurs when a charged particle travels through a dielectric medium. It is usually visible and pre-dominantly at the blue end of the spectrum. The light from each element of the track occurs along the surface of a cone, symmetrical about the axis with a semi-vertical angle θ (Fig. 16).

The angle θ may be found be the relationship

$$\cos \theta = \frac{1}{\beta\mu}$$

where β = v/c for the particle

μ = refractive index of the medium for the particular wavelength.

The cone may be explained by means of the Huyghen construction as shown in Fig. 16.

The seat of the radiation is in the polarization field set up by the particle. At low velocities this field will be symmetrical about the path of the particle, both at right angles and along it, giving no resultant field at a distance. At higher velocities however, due to the finite relaxation time of the field, it will be assymetrical along the axis. When the velocity of the particle is higher than the phase velocity of light in the medium it is possible for wavelets from the resultant field to reinforce as shown in Fig. 16.

Cerenkov radiation should not be confused with Bremsstrahlung. The former arises from distortion of the medium by the particle, the latter from scattering of the particle.

Fermi was able to account for energy loss due to Cerenkov radiation from his theory which considers the flux of the Poynting vector through a cylinder which has the path of the particle as its axis. This flux is equated to the energy loss occurring at distances greater than the radius of the cylinder. This shows that there is a residual radiation at large distances from the track, which is to be identified as Cerenkov radiation. This loss is thus already accounted for in ionization loss theory and is not additional to it.
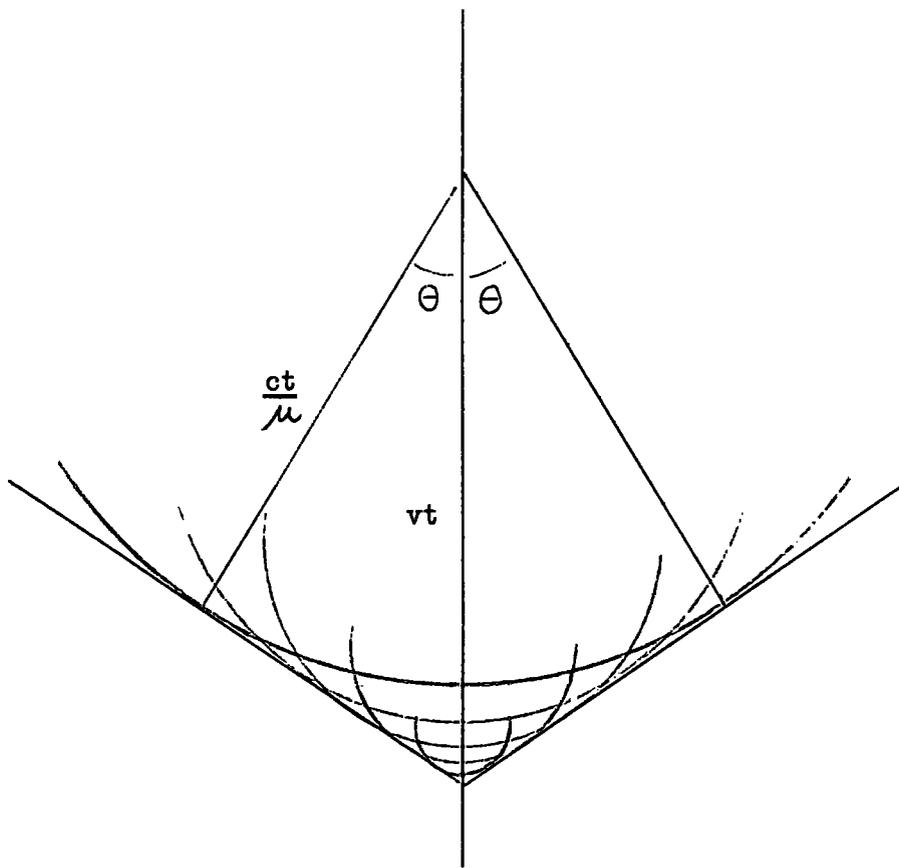
Fig. 16 Huyghen Construction for Cerenkov Radiation.

Other workers showed that, on the basis of Fermi's theory, all of the relativistic increase in energy loss was due to Cerenkov radiation and that there was no increase in true ionization loss beyond the minimum $(\beta^2\ 0.97)$.

This, however, was in conflict with experiment, and Huybrichts and Schönberg (1952) suggested that Fermi's treatment of close collisions was at fault and that modification of the coherence of the radiation by surrounding atoms would cause it to be reabsorbed almost immediately. They concluded that Cerenkov radiation was almost entirely the result of distant collisions.

This line of theory was improved by Fowler and Jones (1953) who showed that, since the dielectric constant was complex in close collisions the Cerenkov radiation would be reabsorbed within 10^{-4} cm of the track.

These methods are essentially artificial in that they consider the medium in two parts, when regarding its structure. The region close to the track is thus taken to have a definite structure while the surrounding medium is regarded as continuous.

The results, though, of these theories are in better agreement with experiment.

5.5. Budini's Treatment

Budini (1953) finds that the separation of the energy loss into energy absorbed in ionization and excitation and that radiated is governed by the ratio

$$\frac{\text{breadth of the spectroscopic lines}}{\text{density of the medium}}$$

The larger this ratio the more favoured is local dissipation.

This is also emphasised by Sternheimer in a different treatment (1952).

In Budini's theory the problem of energy loss is discussed classically by supposing that the absorption bands for ionization pertinent to very broad absorption lines. His results show that:

i) There should be a relationship between the broadness of the spectroscopic lines and the structure of the Cerenkov spectra.

ii) Only an assumption of a perfectly transparent medium leads to results which ascribe all the 'log rise' to Cerenkov radiation, and in this case his formula reduces to that of Frank and Tamm (1937).

iii) There should be simultaneous increases in energy loss by ionization and Cerenkov processes in the relativistic increase region.

5.6. Quantum Theories

There are two quantum theories of the energy loss of fast charged particles, and there are due to D.A. Tidman (1956) and U. Fano (1957).

Fano presents an atomistic dielectric theory by considering three coupled quantum mechanical systems:

    i) an aggregate of atoms

   ii) the long wave components of the electromagnetic field

  iii) additional charged particles.

He derives expressions for the longitudinal and transverse, normal mode excitations in inelastic collisions separately, and shows that the transverse oscillations have a finite probability for relativistic incident particles only and in addition that those whose eigenfrequency is substantially shifted from the excitation energies of the medium, due to coupling with the field, will appear as Cerenkov radiation.

Results from this theory must be computed and as yet none appear to have been published.

Tidman's theory has similar aims but he has adopted a different method. Primarily he is concerned with a quantum theory of refractive index but he has extended this to energy loss and presents his results as the sum of the contributions for the K and L shells of the atom.

Thus results may be computed for the first ten elements in the atomic table.

Both Tidman and Fano give separate expressions for the three different mechanisms of 'ionization' energy loss and Tidman's results for oxygen are shown in Fig. 17b

5.7. Comparison of Results

One of the better experimental tests of these theories was made by Ghosh et al (1952). Thus many of the theories have been calculated for oxygen at N.T.P. (which was used in this experiment). Thus, this provides a convenient method of comparing the theories (Fig. 17a). That due to Sternheimer has been recalculated using the latest values of the constants given by him (1959).

We see that the rise from the minimum to the plateau predicted by Sternheimer is much greater than that given by Tidman's results. This, however, is not sufficient to show that either of the theories is basically incorrect as they both contain constants which must be determined by experiment, and hence the final values predicted by the theories are dependent upon those assumed for the constants.

Budini and Sternheimer's results generally differ in the approach to the plateau, Sternheimer's theory favouring a more gradual approach reaching the plateau at a higher energy.
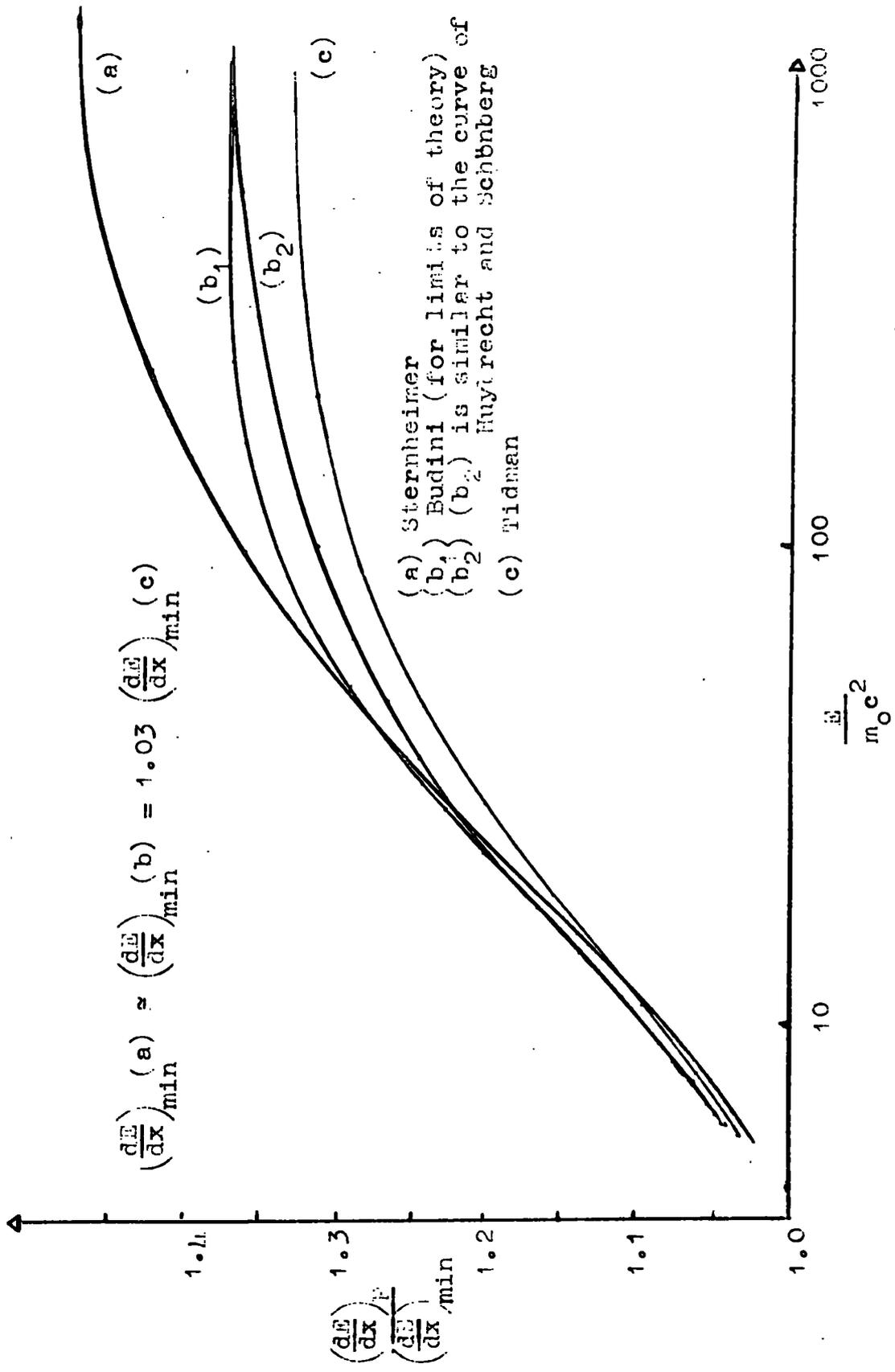
Fig.17a. Theories for Energy loss in Oxygen (at 1 atmos.).
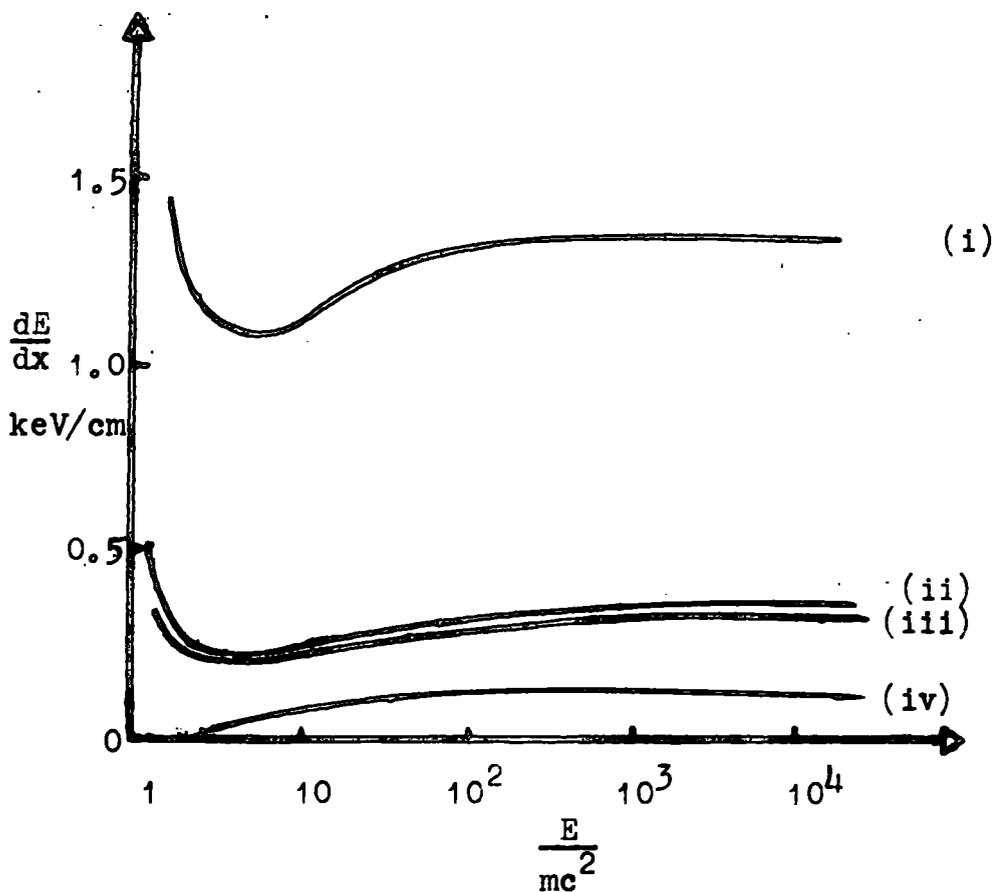
Distribution of Energy Loss by Different Mechanisms

(i) $\left(\dfrac{dE}{dx}\right)$ ionization in distant collision L shell

(ii)   "   excitation   "   "   "   K shell

(iii)   "   ionization   "   "   "   K shell

(iv)   "   Cerenkov   "   "   "   K shell

Fig. 17b. Tidman's Results.
        Energy loss in Oxygen (1 atmosphere)

CHAPTER 6

The Primary Specific Ionization and Energy Loss per

Ion Pair

As was pointed out in Chapter 1, most convenient ways of measuring energy loss do so by measuring the ionization produced, neglecting the fraction of the energy lost producing excitation. In particular some methods measure the primary ionization produced. In In counter work if an absolute value for the energy loss is to be obtained, the apparatus must be calibrated and this is usually done using a radioactive source which causes photoelectrons of known energy to be ejected and stop in the counter. If this method is to be successful, the energy loss per ion pair must be identical both for the charged particles used in the experiment and the calibrating electrons.

6.1. Theories of Primary Ionization

The primary specific ionization, J, measured as the number of ionizing collisions per cm and NTP was first given by Bethe (1933) as;

$$J = 2\pi r_0 mc^2 \frac{NZ}{A} \, a \left[\frac{\ln 2mc^2}{(1-\beta)^2 I(2)} + b - \beta^2 \right]$$

Where a and b are dimensionless constants depending on the gas, and the other quantities are those already introduced in the previous chapter.

Budini and Taffara (1953) have given a value for J in hydrogen and later (1956) gave a more general expression. This is incidental to a theory for ionization loss. They give,

$$J = \frac{2\pi e^4 n}{mv^2} \sum_{k=1}^{z} \left\{ \overline{f}_k \left(\frac{1}{I_k} - \frac{1}{T} \right) + \cdots \right.$$

$$\left. + \frac{1}{2\pi r_0^2 c} \int_{\omega_k}^{\infty} \frac{\sigma_k(\omega)d\omega}{\hbar\omega} \cdot \ln\left[\frac{mI_k\beta^2}{2\pi n r_0 \hbar^2 \omega^2 (1-\beta^2)|\varepsilon_\omega|} - \beta^2 R_e \varepsilon(\omega) \right] \right]$$

Where $\overline{f}_k = \sum_{i=1}^{S} f_{ki} + \sqrt{\frac{n}{r_0 n^3}} \int_{\omega_k}^{\infty} \sigma_k(\omega) d\omega$.

and concerns the probability of transfer between the shells, and

$$\varepsilon(\omega) = 1 + \sum_{k=1}^{z} \left[\sum_{i=1}^{S} \frac{f_{ki}}{\omega_1^2 - \omega^2} + \cdots \right.$$

$$\left. \cdots + \sqrt{\frac{n}{r_0 n^3}} \int_{\omega_k}^{\infty} \frac{\sigma_k(\omega')d\omega'}{\omega'^2 - \omega^2 - \frac{2}{3} i \sqrt{n} r^3 n \omega^3} \cdot \right]$$

In these equations:

e = charge of the electron

v = speed of the incident particle

m = mass of the electron

r_0 = classical radius of the electron

n = no. of electrons/cm^3

Z = atomic number of medium

T = maximum transferable energy

I_K = ionization potential of k'th electron

$w_K = \dfrac{I_K}{h}$

w_i = frequency of i'th absorption line

f_{ik} = oscillator strength of the i'th line of the K shell

σ_K = photo elect. Xsect for k'th electron.

In common with theories of energy loss it is dependent on the values assumed for the constants, especially those for the photoelectric cross-sections.

6.2. Energy Loss per Ion Pair

The energy loss per ion pair which we will denote by Ω includes excitation and Cerenkov losses as well as those directly producing the ion pair. Thus Ω will be greater than the mean ionization potential of the atom. It must be emphasised that the number of ion pairs includes both those due to primary and those due to secondary processes.

Sufficient experimental work (Valentine & Curran, 1959) has been done to show quite conclusively that there is no significant variation in Ω with energy of the incident particle in the case of electrons and particles. But it is not clear that Ω is the same for electrons and α-particles, as experiments conflict on this point.

More work is needed in the case of protons and very little has been done in the case of mesons.

It is clearly not safe to assume that Ω does not vary for different incident particles. This being so, confidence cannot be put in absolute results, determined in this manner, but since there appears to be no variation in Ω with energy we may relate relative numbers of ions produced at different energies to energy loss.

CHAPTER 7

The Most Probable Energy Loss

The energy loss sustained by a charged particle passing through a thin absorber is subject to fluctuations which were first studied by Bohr (1915) and then by Williams (1929, 1931). They showed that the probability of a given energy loss was given by a skew-distribution similar to that in Fig. 2.

7.1. The Transport Equation and Landau's Solution

We denote the statistical distribution function of energy loss by $f(x,\Delta)$ such that this gives the probability that a particle of an initial energy E_0 will lose an energy between Δ and $\Delta + d\Delta$ in an absorber of thickness x. The discussion is limited to those cases where the energy loss is much less than the initial energy. Then the probability per unit path length of a loss of energy between ε and $\varepsilon + d\varepsilon$ $(\omega(\varepsilon)d\varepsilon)$ may be taken to be independent of E, the energy of the particle at any point in the absorber.

We will examine the change in $f(x,\Delta)$ in the interval $x \rightarrow x+dx$, and we see that such a change may be divided into two contributions.

Consider a particular cell of the distribution containing particles which have lost an energy $E_0 - E = \Delta$ in a thickness x. In the interval dx the number of particles in the cell will be increased by particles having an energy greater than E losing further energy and decreased by particles in cell losing energy in the interval. Then giving the two contributions in order;

$$\frac{\partial f}{\partial x}(i) = \int \omega(\varepsilon) f(x, \Delta - \varepsilon) d\varepsilon$$

$$\frac{df}{dx}(ii) = \int \omega(\varepsilon) f(x, \Delta) d\varepsilon$$

Adding;

$$\frac{df}{dx} = \int \omega(\varepsilon) \left\{ f(x, \Delta - \varepsilon) - f(x, \Delta) \right\} d\varepsilon$$

The limits have been omitted (qv). This transport equation may be solved by use of an integral transform.

Landau (1944), using a Laplace transform and taking the limits of the integral as 0 to ∞, finds

$$f(x, \Delta) = \frac{1}{2\pi i} \int_{-i\infty + \sigma}^{+i\infty + \sigma} \exp\left(p\Delta - x \int_0^\infty \omega(\varepsilon)\left(1 - e^{-p\varepsilon}\right) d\varepsilon\right) dp .$$

This requires that $\omega(\varepsilon)$ should be known.

He takes the integral,

$$\int_0^\infty \omega(\varepsilon)(1 - e^{-p\varepsilon}) d\varepsilon ,$$

and splits it into two by defining an energy ε_1 so that

$$\varepsilon_1 \gg \varepsilon_0 \quad \text{and} \quad p\varepsilon_1 \ll 1,$$

and in order that this can be done, $p\zeta_0 \ll 1$, $p\zeta_{max} \gg 1$.

Then

$$\int_0^\infty \omega(\xi)(1-e^{-p\xi})d\xi = p\int_0^{\xi_1} \xi\,\omega(\xi)d\xi$$
$$+ \int_{\xi_1}^\infty \omega\xi_1(1-e^{-p\xi})d\xi.$$

Landau uses the Bethe cross-section for the first term of the integral and the Rutherford cross-section for the second. The distribution he finds is shown in Fig. 2

7.2. Further Solutions

Landau's method has been extended by Symon (1948) to cover the case of absorbers of any thickness, covering the transition from the Landau distribution for thin absorbers to the gaussian form for thick absorber.

Moyal (1955) using a Fourier transform also obtains Landau's results.

Experiments show that Landau's solution does not satisfactorily predict the widths of the distributions which are found. In particular the distributions found for relativistic electrons are much wider than those given by theory. With this in mind Blunck and Leisengang (1950) have modified Landau's method. They include the second moment of the expansion of the exponential in the first term of the equation and show that this increases the theoretical width of the distribution.

Their results agree with those of Landau for higher values of the absorber thickness.

Approximations in Landau's theory, which may cause the discrepancy between theory and experiment, have been pointed out by Hines (1955) and Vavelov (1957) and also by Moyal (1955).

In particular the use of infinity as the upper limit in the transport equation, and in approximate cross-sections which ignore the resonance effect present for large energy transfers to the inner electrons, are such.

Hines solves the transport equation using a Mellin transform specifically for relativistic protons, using an upper transfer limit $\mathcal{E}_{max}$. In common with Vavelov, whose treatment is more general, he shows that the ratio width of the distribution is dependent on the particle energy and that there is no counterpart to Landau's universal curve.

The question of resonance has been examined by Moyal who shows that this would lead to an increase in distribution width. Since his solution retains infinity as the upper limit to the integral it is clear that theoretical difficulties in this field have not yet been completely resolved.

On the lines of Moyal's theory, Rosenweig (1959) has published corrections to Symon's solutions to take resonance into account.

7.3. Conclusions

Although Landau's theory shows little or no agreement with experiment with regard to the width to be expected, quite close agreement may be found between the experimental and predicted values for the variation of the probable energy loss with initial energy although in general experiment yields lower absolute values. For this reason, and for its ease of application, most authors still compare their results to this theory regardless of the fact that it contains conditions which often exclude their experiment from the range of applicability. It is thus used as a convenient yardstick against which the results are displayed.

The relevant condition is that the most probable energy transfers should be much greater than the ionization potentials of the electrons of the material.

The majority of experiments published fail to satisfy this condition, which is inherent in other theories also.

CHAPTER 8

Fluctuations in Pulse Height

The pulse heights recorded on the proportional counter oscilloscope, corresponding to the passage of a particle of given energy across the counter, are subject to fluctuations due to a variety of causes. They are as follows;

    i) Fluctuations in the number of primary collisions and the energy transferred in those collisions.

    ii) Multiplication in the proportional counter.

    iii) The position of the ionization in the counter and the type of track.

    iv) Noise in the proportional counter and associated electronics.

    v) Variations in the amplification of the pulses.

    vi) Observational and recording errors.

In practice by far the greatest contribution comes from the fluctuations in energy loss and fluctuations in the number of primary ions.

8.1. Fluctuations in Energy Loss

As previously indicated the fluctuations in energy loss depend greatly on the thickness of the absorber.

We may then classify the thickness of an absorber by the form of the energy loss distribution which it will produce. It is convenient to make use of Landau's para-

meter ξ where;

$$\xi = \frac{2 Ne^4 \mathrm{p}l}{mv^2} \frac{Z}{A}$$

and e = electronic charge

N = Avogadro's number

m = mass of the electron

v = velocity of the incident particle

s = density of the absorber

l = thickness of the absorber

Z = Atomic No. of the absorber

A = Atomic Weight of the absorber.

Thus ξ is proportional to the number of electrons per sq. cm. and energy transfers of this magnitude constitute the main contribution to the width of the distribution.

Then if I is the mean ionization potential of the atom and E_{max} is the maximum transferable energy, we have,

Class I:- Very Thin Absorbers, $I \sim \xi$

Class II:- Thin Absorbers Landau's Condition $I \ll \xi \ll E_{max}$

Class III:- Thick Absorbers $\xi \sim E_{max}$.

Theory shows that Class III absorbers give rise to Gaussian distributions, and may concern us no further.

The theories reviewed in Chapter 7 are applicable to Class II absorbers, but with the additional condition that we must exclude from the calculation those electron

shells whose potentials are greater than ζ.

No theory exists to cover Class I absorbers. The problem resolves itself into solving the equation.

$$f(x,\Delta) \rightarrow x\,\omega(\Delta) + \delta(\Delta)\left[1 - x\int_0^{\varepsilon max}\omega(\varepsilon)d\varepsilon\right] \text{ as } x \rightarrow 0$$

8.2. <u>The experimental results on distribution width for</u>

<u>thin and very thin absorbers</u>

The experimental width as measured is usually expressed as a percentage of the most probable energy loss. According to the Landau and other theories the width is not proportional to the most probable energy loss for a given absorber. Thus we may not compare, profitably, the percentage widths found for the same particles of different energy. It is convenient to consider the width of the distributions produced by minimally ionising particles ($\beta \cong 0.9$) since there are sufficient experimental results available. This was done by West (1953) and his results are shown in Fig. 18. He shows in his paper that the different gas absorbers may be considered together by the use of the parameter Π which is the product of the track length and the pressure of the gas filling. For a given value of this constant all counter fillings give approximately the same width for the distribution.

It is easily shown that $\zeta/I_0 Z$ is an equivalent parameter.

A similar investigation with μ-mesons was made by Palmatier, Meers and Askey (1955) and their results are similar in character to those found by West (Fig. 19)

The rise in the width found for low values of Π may be attributed to resonance effects, but it can be seen that Landau's theory predicts widths which are too small even for high values of Π.

We may ascribe this deficit in part to the fact that the theory deals with fluctuations in energy loss and not in ionization as measured.

This is particularly important in the case of absorbers where $\xi < I$ for the inner shells. Effectively a width applicable to the total energy loss is associated with that loss for shells where $\xi > I$. Thus the percentage width of the observed distribution is larger than that predicted by theory.

Eyeons (unpublished) has shown by a semi-empirical method that the width of the distribution is given by the relationship

$$(\text{Width})^2 = \text{constant} + \frac{\text{constant}}{\text{Gas Pressure} \times \text{Path Length}}$$

This is compared to experimental results in Fig. 20 and Palmatier's results are shown similarly.
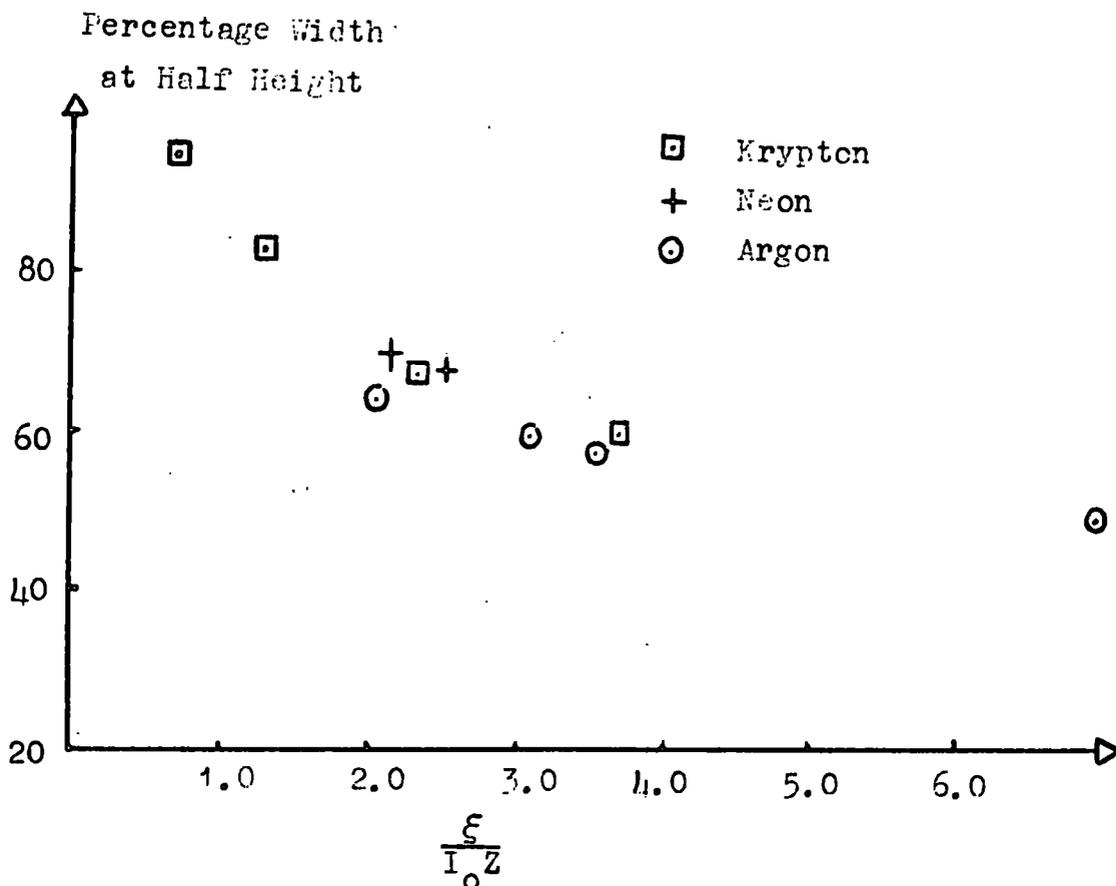
Fig. 18. West's Results for Minimally Ionizing Electrons
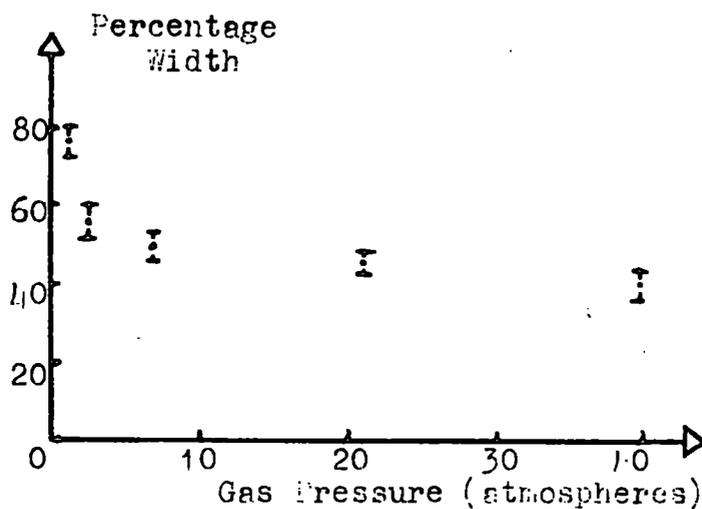
Fig. 19. Palmatier's results for Minimally Ionizing
μ-mesons.
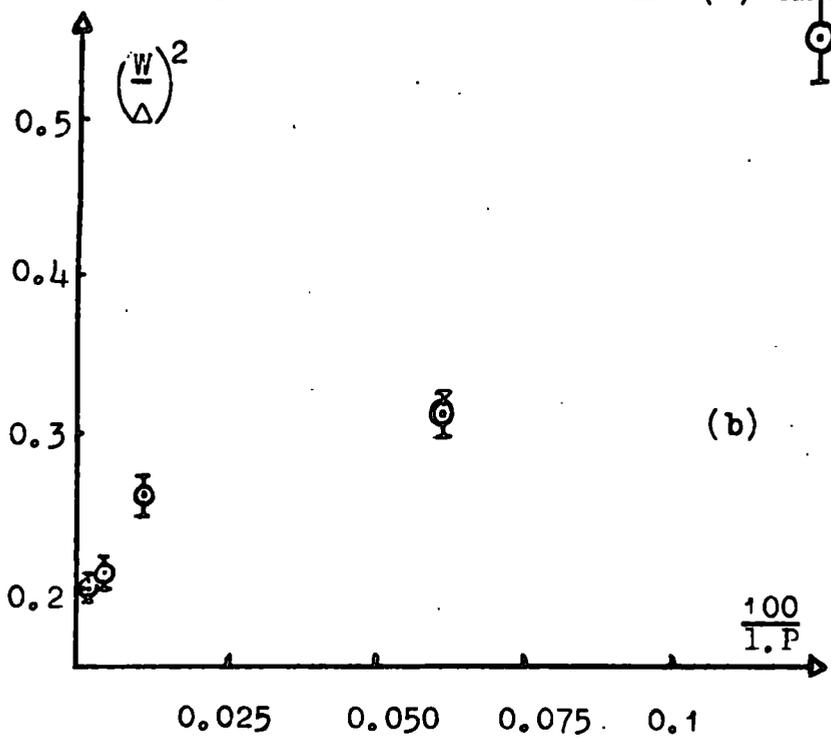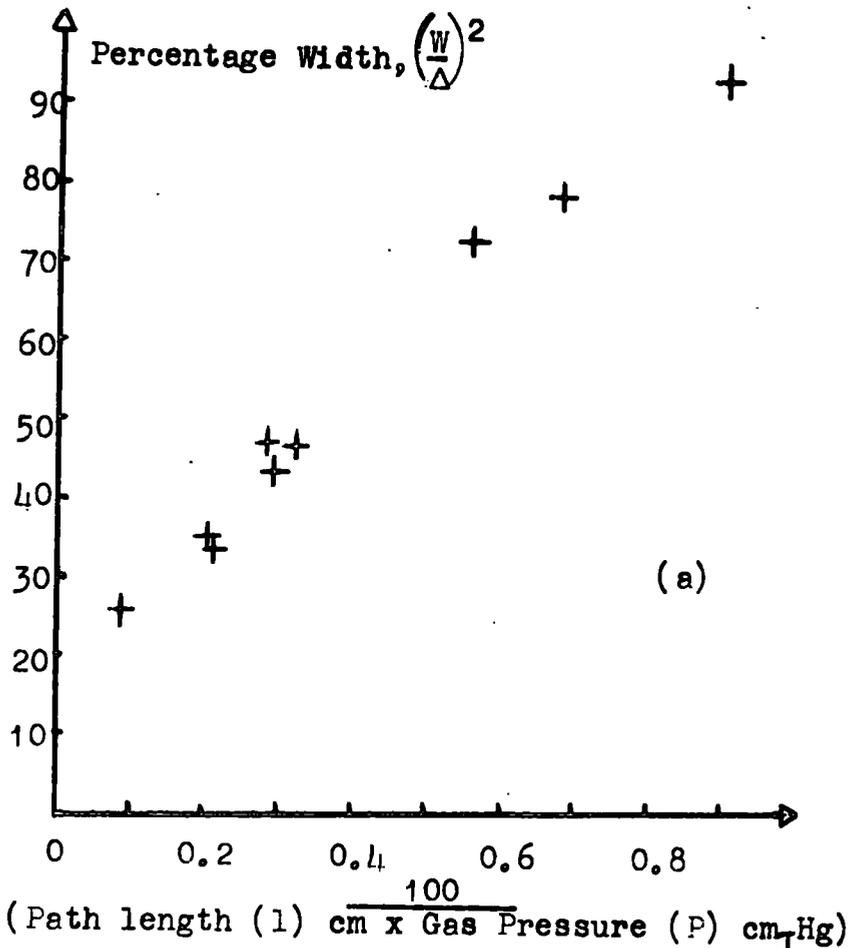
Fig. 20 West's (a) and Palmatier's (b) Results.

8.3. <u>Statistical Spread in Pulse Size in a Proportional</u>
<u>counter for a given energy loss.</u>

The theory of Frisch (1947) and the experiments of
Hanna, Kirkwood, and Pontecorvo show that the relative
variance (the mean square standard deviation) of the
output pulse size is practically independent of the
multiplication factor.

Then
$$\left(\frac{\sigma_P}{\overline{P}}\right)^2 = \frac{1}{N}\left(\frac{\sigma_A}{\overline{A}}\right)^2 + \left(\frac{\sigma_N}{\overline{N}}\right)^2$$

where $\left(\frac{\sigma_P}{\overline{P}}\right)^2$ is the relative variance of the output pulse
size,

$\left(\frac{\sigma_A}{\overline{A}}\right)^2$ gives the relative variance in the number of
ions produced in an avalanche by a single
ionization electron,

$\left(\frac{\sigma_N}{\overline{N}}\right)^2$ the relative variance in the number of initial
electrons.

The variation in the multiplication process was
given by Snyder and Frisch (1950), where each collision
is assumed independent of the previous history of the
electron, as $\frac{1}{N}$ (where N = no. of primary electrons).

Their assumptions will not be completely satisfied
in practice and the experiments of Curran, Cockcroft and
Angus showed that

$$\frac{1}{N}\left(\frac{\sigma_A}{\overline{A}}\right)^2 = \frac{0.68}{N}$$

Fluctuations in the initial number of ions have been investigated theoretically by Fano (1947) who estimates that

$$\left(\frac{\sigma_N}{\overline{N}}\right)^2 = \frac{1}{\overline{N}k}$$

where $2 < k < 3$. The resulting distribution is symmetrical.

8.4. Other contributions

The final observed distribution will be further widened by errors associated with experimental technique.

The effect of ionization position in the counter has been examined by Hussein and Jaffe (1959) and they show that the fractional variation of the pulse height is $\frac{1}{A}$ where A is the amplication factor. Their treatment assumes that electron collection all takes place before the positive ion sheath moves. Where recombination occurs this assumption is not satisfied and the resultant width would be greater.

Finally fluctuations in apparatus performance and errors in analysis will contribute a few per cent to the width of the final distribution.

CHAPTER 9

The Experimental Results

The results for the ionization loss of μ-mesons in the proportional counters are obtained from the apparatus as pulse heights on an oscilloscope screen. These may be grouped into histograms for each category and then represent the nearest experimental equivalent of the Landau distribution. The conclusions to be drawn from these histograms, regarding both the value of the mode and the width of the distribution, depend on the performance of the apparatus, particularly with respect to its linearity and stability.

9.1. The Stability of the Apparatus

The performance of the proportional counter is strongly dependent upon the E.H.T. voltage supplied in that a small change in this quantity gives rise to a relatively large change in the amplification produced in the counter by the multiplication process.

In this experiment, a fraction of the E.H.T. voltage was regularly compared with a Weston Cadmium Cell by a potentiometer method.

The measurements showed that, after switching on, the pack gives a voltage steady to within 0.2% after a period of 12 hours. This is sufficiently stable with regard to the multiplication variations in the counter (q.v.).

The head - and main - amplifiers are commercial units with a stated stability of 1%. The whole pulse amplification chain, including the proportional counters, remained steady, as measured by the distribution due to the calibrating sources, given on the Pulse Height Analyser, with a possible variation of 3-4%. Some of this is due to the P.H.A. itself.

The proportional counter oscilloscope showed no visible variation in heights corresponding to standard pulses.

9.2. The Linearity of the Apparatus

The linearity of response of the proportional counter may be affected, as indicated in Chapter 3, by interference between individual 'avalanches' in the multiplication region. That this defect was not present in this experiment is shown by the use of two sources, one of which released more electrons in the counter than would normally be of interest during the experiment, and further by measurements of the change in amplification produced by changes in the voltage supplied to the counter.

The theoretical ratio of the energy losses by the two sources is 3.01. The measured ratio was 3.0 ± 0.08.

The pulse heights for one source for varying values of the E.H.T. were as follows:

E.H.T. Voltage	pulse height volts
965	4
1060	8.5
1145	21

Table 1. Variation of Pulse Height with E.H.T. for Zn Source.

Thus we may conclude that under the operating conditions there is no saturation occurring in the proportional counter, nor indeed, throughout the amplification chain.

We also see that the variation of amplification with voltage $\frac{dA}{dV} \lesseqgtr 1.25\%/v$. It follows then that the E.H.T. variations (Section 8.1) lead to a possible error of 0.25% in the pulse heights recorded.

The amplifier used is 'linear within 1%' for output pulses up to 50v. The voltage corresponding to the most probable energy loss in the counter is $about \ 10v$

The proportional counter oscilloscope records pulses linearly up to $15v$ (The value for the most probable loss is $5v$). The attenuation between this oscilloscope and the amplifier was also found to be linear.

9.3. <u>Measurements using the X-ray Sources</u>

Results using the two radioactive Sources are given in Appendix II

Here measurements quoted in the previous section
are detailed together with the pulse height distributions
for each source under different conditions of amplifica-
tion.

The latter results show that the distribution for
complete energy loss within the counter is symmetrical
as expected from theory.

9.4. <u>The Analysis of the Film Results</u>

The Film results of the pulse produced by a given
particle and its category number are recorded on separate
films and typical results are shown in Fig. 14.

The films (35 mm) were first analysed under the
following headings

<u>Film 1</u>

Time	Proportional Counter			Double Pulse (reject)	Pulse Height mm.
	A	B	Double		

<u>Film 2</u>

Time	Category Number 0 - 15		+_	Knock-on

This analysis was performed using a micro-film reader,
giving pulse heights of about 30 mm. These were measured
with an accuracy of 3-5%. Both of these film analyses
were recorded on the same sheet.

After rejecting all 'double' and 'knock on' events a second analysis folowed which listed the pulse heights for each category and each counter separately. Then histograms showing the numbers of pulses corresponding to different pulse heights were found.

At this stage precautions were taken to ensure that no results were included where correlation between the two films was suspect. The pulse height histograms for all pulses from each counter were formed. The ratio between the maxima of these distribution was compared to the known ratio of the amplifications produced by the counters. Unless these ratios were the same within experimental error the results were discarded. Some shorter films had insufficient particles for this test to be accurate, and results on these films were not used.

In the satisfactory cases the results from one counter were multiplied by the relevant factor and added to those of the other counter.

There are basically two sets of results depending on the value of the magnetic field used in the spectro-graph. For both these sets the amplification through the system remained the same and thus the results for the two films are directly comparable.

9.5. Mean Momentum for each category

The histogram results will give the most probable pulse height for each category. So that the dependence of pulse height on momentum can be found the effective mean momentum for each category must be found.

This may be done accurately by the following method.

i) Assume the correct form for the Landau distribution.

ii) Multiply by the differential momentum spectrum for the category.

iii) Compare with the experimental distribution.

iv) On the basis of this comparison modify the assumed distribution.

This procedure should be repeated until the experimental distributor is correctly predicted.

This method would also yield an energy loss distribution which could, after correction for width introduced by the apparatus be compared with theory.

However, as, so far, a large number of particles have not been recorded, a shorter approximate method was preferred. This involved multiplying the category momentum distribution by a theoretical ionization-momentum relationship. The validity of this procedure may be argued as follows. The variation between the mean momentum calculated before multiplication by the ionization relationship, and that after, is small. Thus so long as the experimental points have a fairly close agreement with

the assumed relationship between ionization and momentum we may expect to have introduced little error.

We must however allow for the fact that we have only a limited number of particles in each category and the expected momentum distribution within that category will not be perfectly satisfied.

Let us suppose that there are N particles in the category. Of these N/2 are above the mean momentum and N/2 below. The deviation in each of these numbers is $\pm \sqrt{N/2}$, the combined error being $\sqrt{N}$

If $N(\bar{\Delta})$ is the value of the deflection distribution at the mean Δ and $\delta\Delta$ is the error in the mean deflection (where the function is normalised so that for the category $\int N(\Delta)d\Delta = N$.

Then $N(\bar{\Delta})\delta\Delta \simeq \sqrt{\dfrac{N}{4}}$

The values for the effective mean momenta for the categories are as follows.

Category	0	1	2	3	4	5	6,7	8,9	10-15
$\bar{p}$ High field	19.35	9.2	4.58	3.06	2.29	1.83	1.44	1.09	0.82
$\bar{p}$ Low field	4.7	2.55	1.3	0.91	0.7		0.56	0.44	

Values in $\text{Gev}/_c$.

The momentum $p = k/_\Delta$

For High field k = 17.42 Magnet current 57.2 amps.

Low field k = 4.98 " " 12 amps.

9.6. <u>Methods for determining the most probable values of the distribution</u>

The prime difficulty of this and other methods of measuring the variation of energy loss with total energy is that the most probable value must be determined from a 'skew' histogram which may not contain a large number of observations, and this problem has in the past received considerable attention.

The many treatments may be divided into three broad classes.

a) Methods involving the assumption of the theoretical distribution.

b) Those whereby the experiment is so modified as to yield a non-skew distribution.

c) Transformations of the distribution which will also give a symmetrical distribution.

The first type of analysis, in different forms has been given by Behrens (1951), Yeliseyev (1953), Palmatier (1955) and Alikhanov (1956). Perhaps the best of these methods however is due to Hammersley and Morton (1954), whose treatment gives more weight to observations near the peak of the distribution and little to those far from it, especially those representing the larger energy losses in which little reliance can be placed.

The second form of treatment relies on the following arguments.

Suppose that the maximum amount of energy lost in the counter is chosen so that the average energy loss is equal to the most probable.

If $\varphi(\Delta)$ is the Landau-type distribution and Δ is the energy loss

Then
$$\frac{\int_0^{\Delta_{max}} \Delta \, \varphi(\Delta) \, d\Delta}{\int_0^{\Delta_{max}} \varphi(\Delta) \, d\Delta} = \Delta_{prob}.$$

where Δ_{prob} is given by the value of Δ for which $(d/d\Delta)(\varphi(\Delta)) = 0.$

Thus if the appropriate fraction of results is rejected the remainder must be averaged to find the most probable value. To determine this fraction however a theoretical distribution must be known or assumed.

Alternatively, each particle may be required to traverse several counters and give rise to N results for energy lost. If the higher of these values are discarded the final distribution composed of the results from several particles will be 'sharpened up' to a symmetrical form, again with the advantage that the average value would then nearly coincide with the most probable energy loss (Alikhanov 1956 Palmatier 1955).

Finally the energy loss distribution may be transformed into a symmetrical curve, either mathematically

or graphically. A logarithmic transformation has been found satisfactory. Graphically the distribution is plotted against the logarithm of energy loss.

A further method has been reported by Barnaby (1961). He found that when the distributions of energy loss of μ-mesons in a scintillator were plotted against reciprocals of the pulse height, approximately normal distributions were found. On plotting the cumulative percentage frequencies against the reciprocal height (on arithmetical probability paper) a straight line is obtained (Fig.   ). The peaks of the distributions were given by the points on the lines where ordinates correspond to 50% on the probability paper.

This procedure is particularly valuable when used to determine the relative values of the probable energy loss as opposed to absolute values.

In the present experiment there are further difficulties complicating the problem of analysis. The categories contain particles with differing momenta, and the range of momenta changes both in width and mean value with category. This means that it is difficult to justify the assumption of one distribution function to cover all categories. Further the relatively small numbers of particles as yet recorded hardly merit the time taken by an objective analysis. The peaks of the distributions have been judged by eye. The author claims

that provided all the distributions are so judged before any attempt is made to group the results in a final ionization loss-total energy relationship, this will not lead to any great subjective errors. It is extremely difficult to mentally relate the distribution to the final relationship.

An estimate of the error was made by approximating the distribution to the normal form by cutting off the high energy tail. If N is the total number of observations remaining and W is the measured helf height width the error was taken as $W/\sqrt{N}$.

9.7. The Experimental Results

Some of the experimental distributions found are shown in Fig. $21a$, and all the distributions are summarised in Table 3 and Figs $21a, 21b, 21c$.

These give the final results showing the relative variation of the most probable energy loss with energy, with respect to the minimum value. These are compared to a theoretical curve calculated from Landau's theory by Sternheimers correction for the density effect. The calculation of this curve is outlined in Appendix III
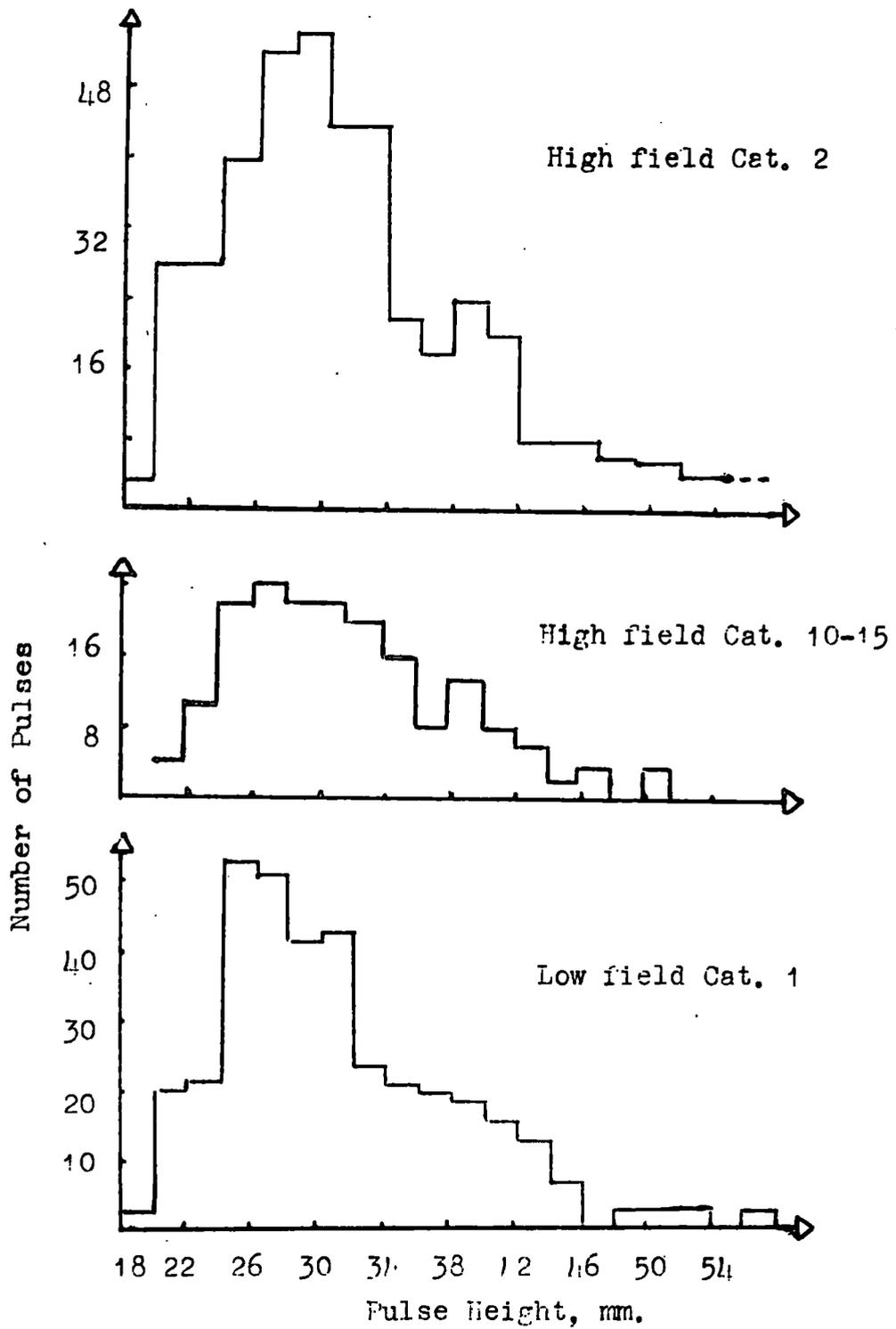
Fig. 24 Typical Category Pulse Height Distributions

Category No.	Mean Momentum Gev/c	Number of Particles	Most probable Pulse Height	Error
High Field				
0	19.35	160	33.5	1
1	9.2	460	31.2	0.6
2	4.58	470	28.8	0.6
3	3.06	420	27.4	0.6
4	2.29	320	26.6	0.7
5	1.83	240	25.8	0.8
6,7	1.44	330	25.7	0.7
8,9	1.09	180	25.2	0.85
10-15	0.82	200	23.6	0.8
Low Field				
0	4.7	293	29	0.7
1	2.55	366	26	0.65
2	1.3	210	25.5	0.8
3	0.91	120	24	1.0
4,5	0.7	101	23.5	1.2
6,7	0.56	51	23	1.5
8-15	0.44	45	23	1.8

Table 3a

Experimental Results.

Category No.	Mean Momentum Gev/e	No. of Particles			Most Probable Pulse Height			Combined Error
		RH.W.	DGJ	Comb.	RH.W.	DGJ	Comb.	
High Field								
0	19.35	90	71	160	34	33.1	33.5	1.0
1	9.2	220	241	460	31	31.4	31.2	0.6
2	4.58	210	256	470	28.5	29.0	28.75	0.6
3	3.06	200	218	420	27.5	27.3	27.4	0.6
4	2.29	150	171	320	26.5	26.7	26.6	0.7
5	1.83	110	130	240	25	26.7	25.8	0.8
6,7	1.44	150	182	332	26	25.5	25.7	0.7
8,9	1.09	85	96	180	26	24.4	25.2	0.85
10 - 15	0.82	100	108	200	23.5	23.8	23.6	0.8
Low Field								
0	4.7	293			29			0.7
1	2.55	366			26			0.65
2	1.3	210			25.5			0.8
3	0.91	120			24			1.0
4,5	0.7	101			23.5			1.2
6,7	0.56	51			23			1.5
8-15	0.44	45			23			1.8

R.H.W. - Present Experiment

D.G.J. - Jones's Result
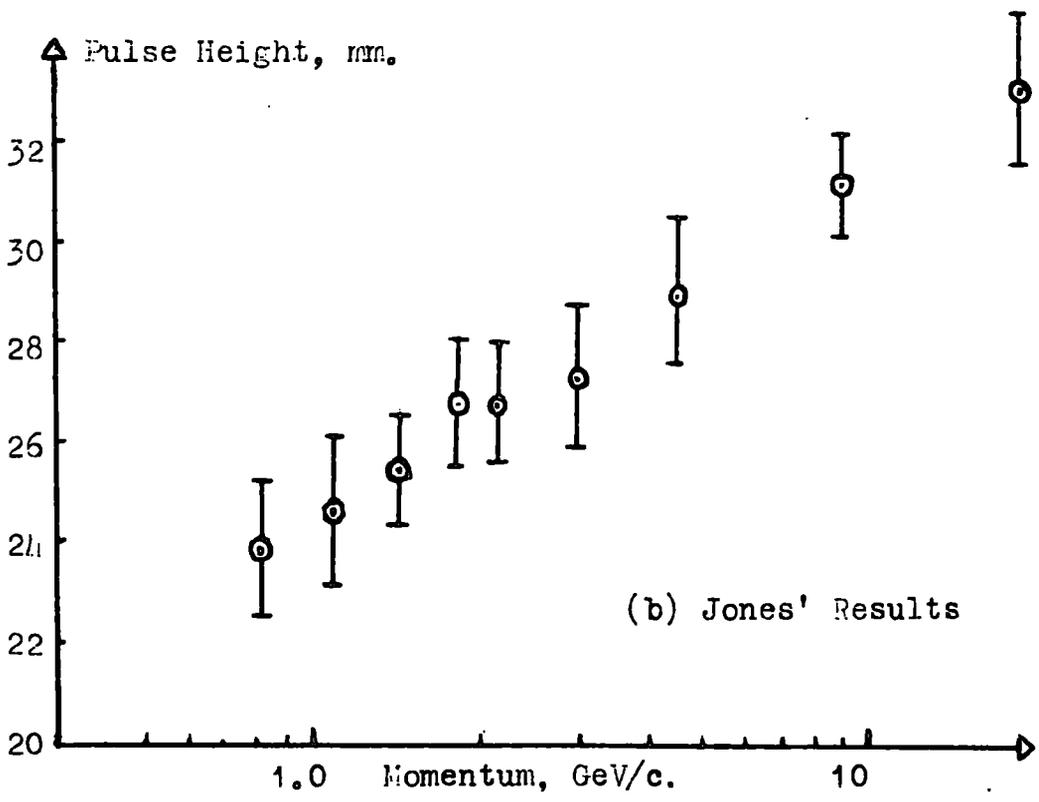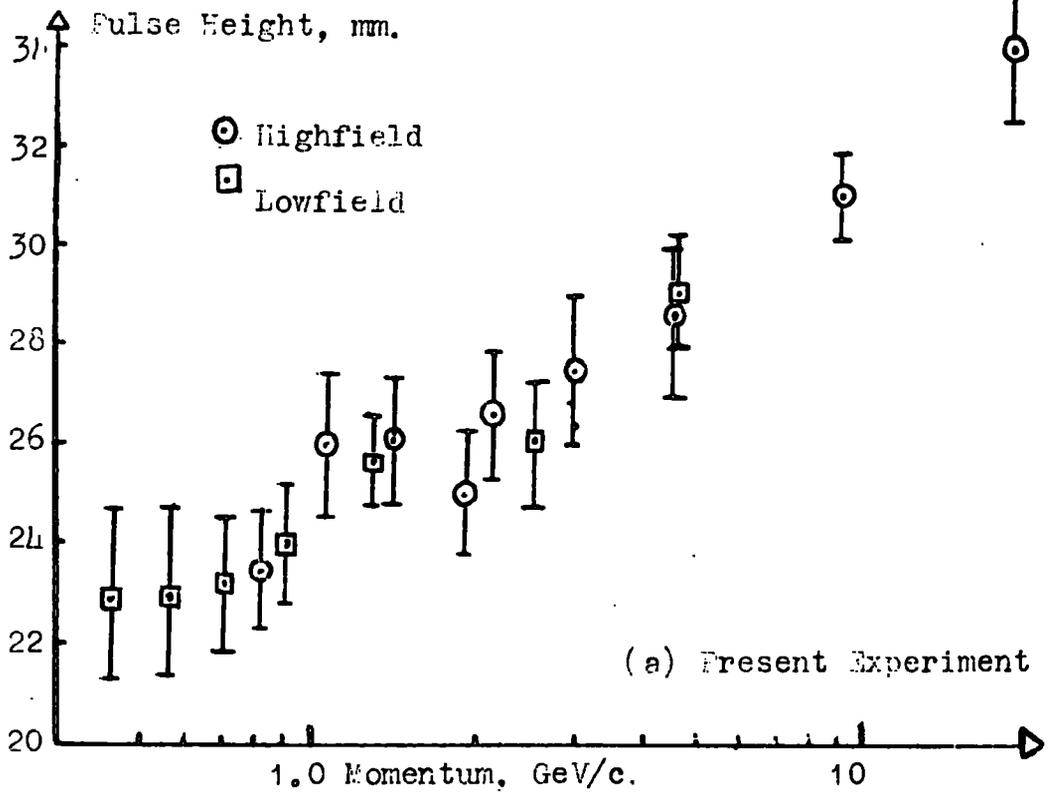
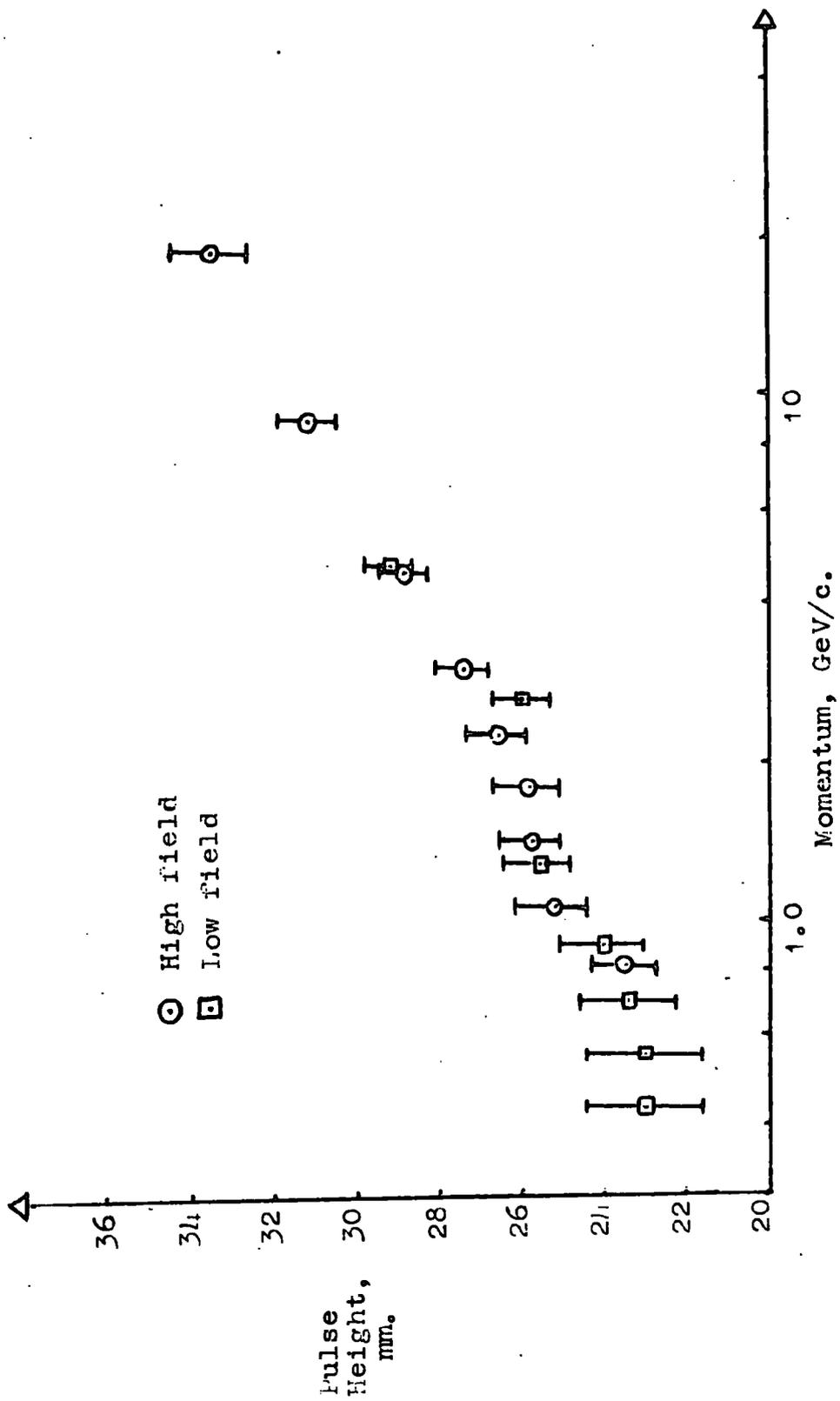Table 3b Experimental Results.

Fig. 21b Experimental Results

Fig. 21c. Ionization Pulse Heights for μ-mesons in 40 cmHg Neon and 3 cmHg Methane. Combined Results.

CHAPTER 10

Recent Work on Energy Loss by Fast Charged Particles in Gases.

Only work published since the review by Price (1955) will be outlined here. The bulk of this later work has been done using cloud chambers and there have been three thorough experiments Two of these have measured total ionization and one, the most recent, primary ionization. In addition one experiment has used proportional counters. Further experiments, mainly with counters, have been directed to investigating the width of the 'Landau' distribution.

10.1. Cloud Chamber Experiments

Both the experiments of Rousset et al (1959) and Kepler et al (1958) measured the average total ionization loss in noble gases, both in single gases and mixtures. The results are similar in that in the case of mixtures there is marked disagreement with Sternheimer's theory, the experiments showing a lower plateau value. The most likely explanation of this difference is that the theory does not accurately take into account interaction between constituents when polarization is being considered. Thus excitation frequencies in the heavier one constituent may give rise to resonance polarizating preventing some elec- trons in the other gas or gases from participating in the

ionization increase. Typical results from each experiment are shown in Fig. 23.24

The other cloud chamber experiment by Fortuȵ (1960), measuring primary ionization shows even great disagreement with theory but in the opposite sense (Fig. 22.). Here it is difficult to say whether the experiment is not in fact measuring primary ionization or whether the density effect predictions of theory are again incorrect.

As these three experiments use the cloud chamber to measure the energy of the particle electrons must be used to obtain plateau energies. In this connection the 30 GeV/c resolution claimed by Kepler et al is remarkable especially when achieved with a diffused track (vide Chapter 3).

In each case the rise from minimum to plateau is covered only by the use of μ-mesons and electrons. These results are compared to a curve calculated for heavy particles. This detracts from the value of the experiments.

10.2. Proportional Counters Work

Only one experiment using counters which covers a range of particle energies has been published since 1955, and then with low statistical accuracy. This is due to Lanou and Kraybill (1959). Their counters were filled to 2.7 atmospheres with 95% He 5% Co_2 and their results are shown in Fig. 25.
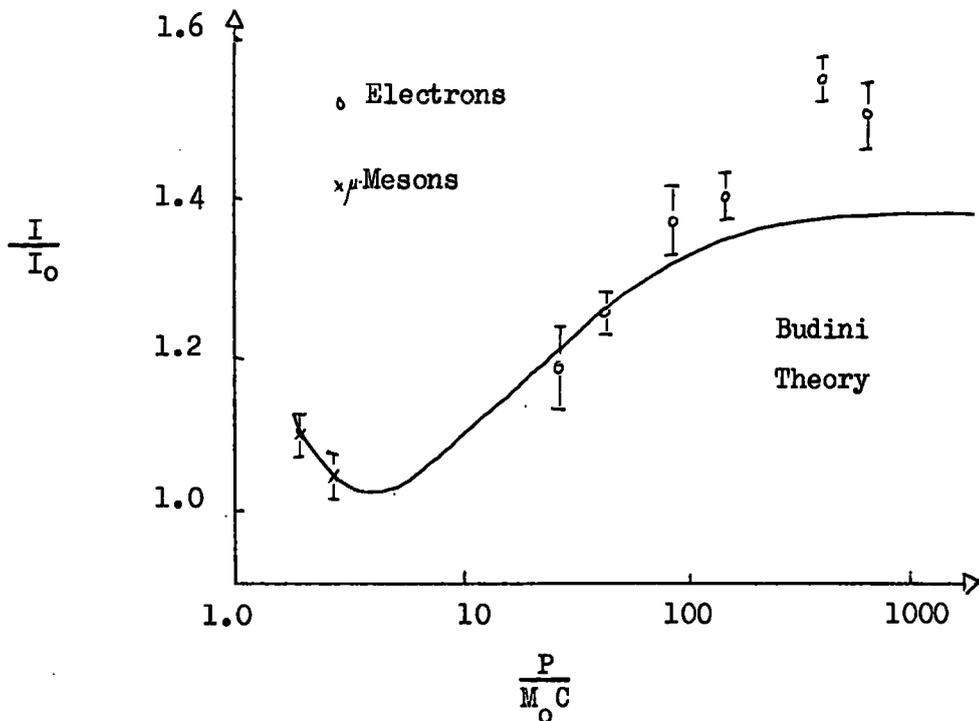
Fig. 22. Results of Fortune

Relative Primary Ionisation in Helium (814 mm Hg)

Constituents	z prob. / ≤ min	
	Calc	Expt.
19 mm Hg Xenon 4 mm Hg Alcohol	1.69 ± 0.03	1.69 ± 0.05
15 mm Hg Xenon 25 mm Hg Hydrogen 4 mm Hg Alcohol	1.65 ± 0.03	1.72 ± 0.05
15 mm Hg Xenon 25 mm Hg Helium 4 mm Hg Alcohol	1.66 ± 0.03	1.33 ± 0.04
14 mm Hg Xenon 50 mm Hg Helium 4 mm Hg Alcohol	1.60 ± 0.03	1.25 ± 0.05

Fig. 23   Rousset   ~~Lanou~~ et al   Ionization by Electrons.
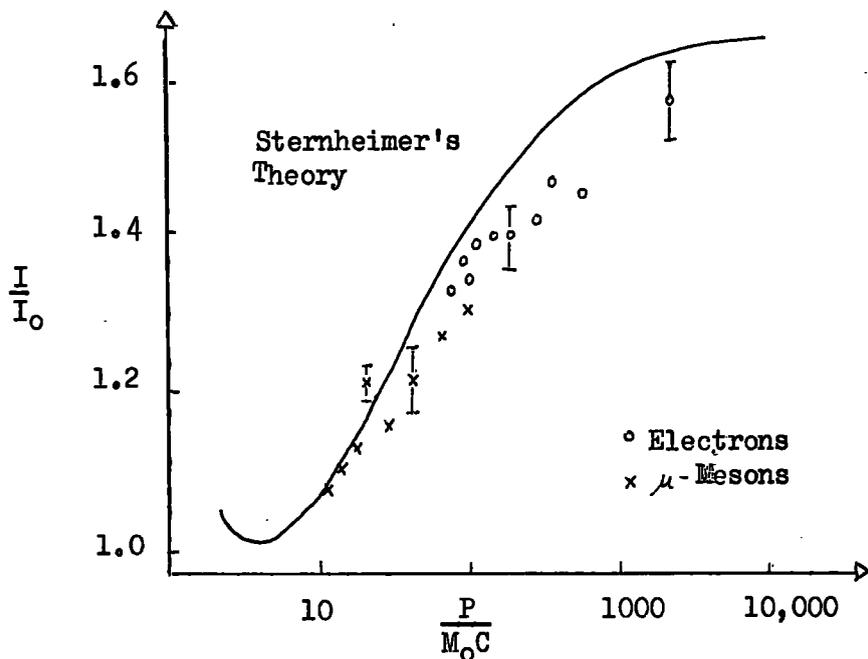
Fig. 24.   Results of Kepler et al.
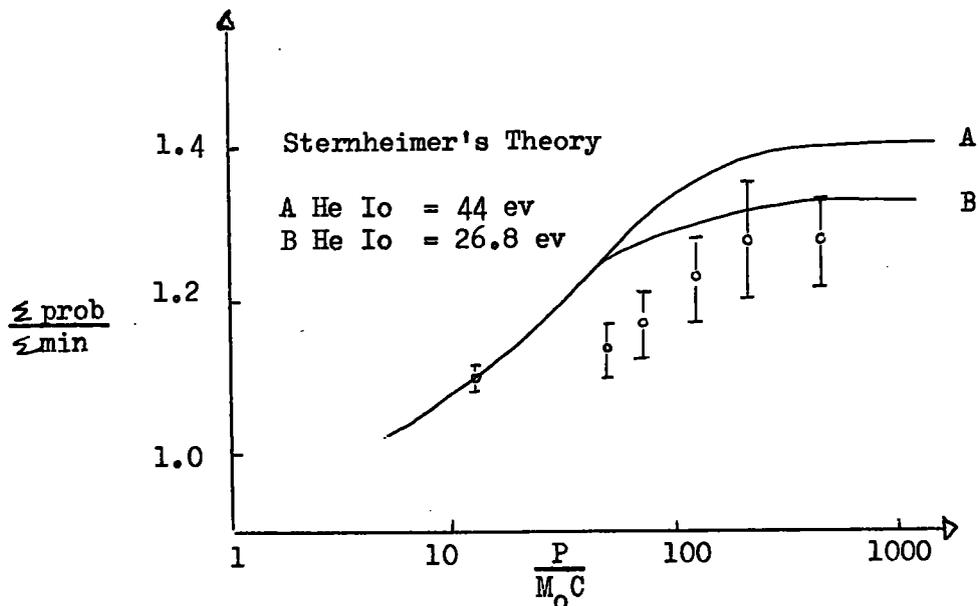
Ionization in an Argon-Helium Mixture.

Fig. 25.   Results of Lanou & Kraybill

Ionization in Helium-CO_2 Mixture.

Gooding and Feisberg (1951) and Igo and Feisberg (1954) have measured energy loss value and distribution for protons in argon. The protons had energies in the range 30-40 MeV. Both experiments show that the experimental width of the distribution is greater than that predicted by Landau's theory.

10.3. Ionization Chambers

W.C. Barber 1956 using electrons from a linear accelerator and an ionization chamber has investigated energy loss in both hydrogen and helium from the minimum to the commencement of the plateau region. The gases were at a pressure of 10 atmospheres. His results show that there is a possibility that the experimental density effect is greater than that predicted by Sternheimer.

10.4. Conclusions

There has been no published experiment sufficiently accurate to verify any particular theory over the complete range of interest (i.e. from below the minimum to the plateau region) where one type of particle has been used.

Secondly, although in nearly every case there is agreement between experimental and Sternheimer's density effect within experimental error, when all experiments are considered there seems to be some evidence that a

greater density effect exists than predicted.

CHAPTER 11

Conclusions.

It has been shown that, although in its present form the experimental arrangement is not satisfactory and that a modified technique would be beneficial, results as good as those of other workers could be obtained for μ-mesons.

In view of the results of Fortune (1960) it would appear that the determination of the primary ionization by means of a cloud chamber presents considerable difficulties in obtaining conditions relevant to present theoretical treatments. It seems unlikely that existing theories are as far from the correct values as the experiment would indicate.

Whereas the case for using proportional counters is thereby reinforced more work is required in the determination of primary specific ionization both by the cloud chamber and low pressure counter methods.

The results of Kepler et al (1958) and Rousset et al (1959) and also the review of Valentine and Curran (1959), concerning energy loss per ion pair indicate that there is interaction between the energy losses processes in the different components of a mixture of gases which is not taken into account in theory especially at high energies. In an attempt to accurately verify any particular theory

allowances would need to be made for this effect or preferably either a mixture should be chosen where such interaction seems unlikely or a single gas should be used.

The Proportional Counters

The counters used in this experiment could be much improved upon, in respect of their construction, filling, and the rate at which information is gathered. These three considerations are to some extent interdependent.

The counters in their present form have a cross-section where the depth is considerably greater than the width. This leads to low field regions in the counter where recombination may occur with deleterious effects on the proportionality of response and the width of the resultant distribution.

There are no precautions to eliminate 'end effect' in their operation and there is insufficient provision for calibrating the counter in the variety of positions necessary.

Filling the counter is a difficult operation and possibly the widely differing amplification properties of counters ostensibly alike may be due to this problem.

All of the counters had deteriorated within six months of filling.

The present gas filling, at about half an atmosphere pressure falls well below the lower boundary condition for application of probable energy loss theory, and but for the wide spread agreement among experimental workers to ignore this breach there seems little to justify it.

A high pressure is required to adequately satisfy the condition but we may base our choice on two other considerations. From the results of West and Palmatier (Chapter γ) it is seen that, for a given counter size, after a certain value a further increase of pressure does not provide a significant decrease in the width of the distribution. Secondly it would be advantageous if the density of the gas were such that the 'density effect' begins to act at about 10-15 GeV/c. This would mean that this region of interest could be studied with greater accuracy and the plateau established in a shorter time than at present possible since the number of particles recorded drops off sharply above 20 GeV/c. It must be remembered though that the voltage applied to the counter must be increased for a given amplification if the pressure of the gas is increased.

A significant increase in the rate at which information is gathered would be enjoyed if the counters were to be placed in the magnet gap of the spectrograph. In

this position, if more than one counter were to be
used, vertical stacking would be necessary. With
this in mind, in addition to the requirement of a square
cross-section to reduce the low field regions a 'multi-
counter' commends itself (Fig. 26.) (e.g. Alikhanov,
1956).

This would consist of a large rectangular metal
box, divided into sections by perforated metal formers,
each section forming the cathode for an individual
counter, the anode in the form of a fine wire is being
stretched along the long axis of the box. The fact
that the multicounter may be more difficult to construct
would be offset by the saving of effort in filling the
counter.

Alternatively, if the counter is to be used for
some time in obtaining results at high momenta with high
statistical accuracy, some means of purifying the fill-
ing may be worthwhile and easier in the case of a
multicounter.

In such a case it would be easier as well as theor-
etically more satisfactory to use a single gas filling,
either methane or propane.

Provision would be necessary for the calibration
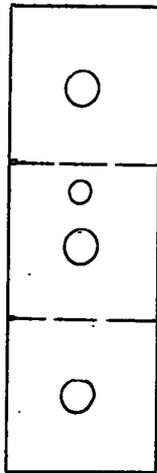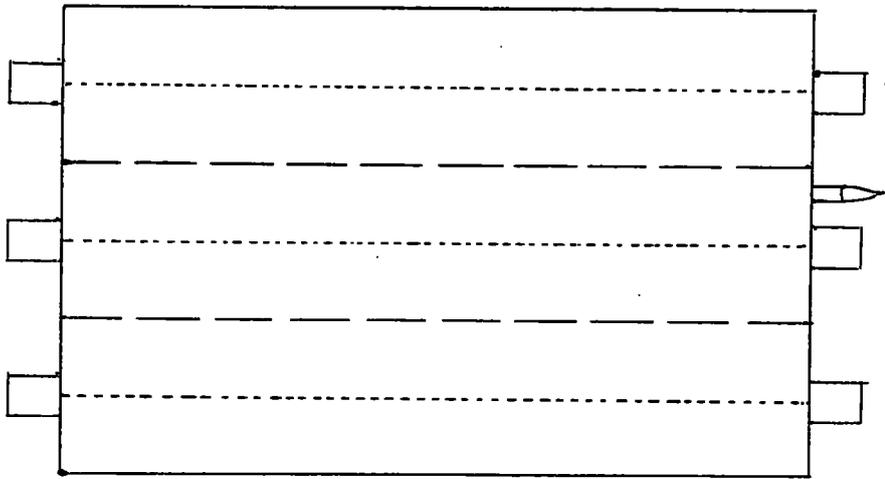of the multicounter in all its sections and throughout
its length.

Fig. 26. Proportional Multicounter
(Three compartments with perforated partitions)

Vertical stacking means that the existing method of recording the results could not be used. In fact this method has proved very unsatisfactory. The use of two oscilloscopes and the resulting separate films have given rise to difficulties of correlation and have greatly increased the time required to analyse the results. If one counter is used it is imperative that both the pulse height and the category number of the particle should be recorded on one film. This could be done using a double beam oscilloscope. With the multicounter the pulses would have to be spaced to make the use of the oscilloscope possible. Otherwise a modified form of the pulse height analyser would be necessary. If this were so these results would have to be combined with the category number from its screen by an optical arrangement, or the momentum analyser would require modification so that each category could be shown by an indicator bulb. The latter course would almost certainly be preferable.

Summary

Despite the need for modification the experiment is capable of providing statistically good results for the ionization energy loss of μ-mesons from the minimum region to points well on the plateau. A multicounter should be used filled to 100 cm Hg. pressure with methane and preferably with some means of purifying the

filling.

The results so far obtained are in agreement in their general features with those of other workers in this field, but, in common with other experiments, are not yet based on sufficient observations to distinguish between different theories.

The advent of the new proton synchrotrons at CERN and elsewhere may render this experiment unnecessary except at very high energy (>30 GeV).

ACKNOWLEDGEMENTS.

APPENDIX I

THE PROPORTIONAL COUNTER.

a) Field in a Rectangular Counter.

The field pattern of the counters used in the present experiment was determined graphically and the results are shown in Fig. AI.1

In thus finding the field two criteria have to be satisfied.
i) that the lines of electric intensity should cross equipotentials at right angles.
ii) that the separation of the equipotentials should be consistent with the corresponding density of lines of electric intensity.

The reasonable assumption was made that the equipotentials would be concentric with the anode at small distances from it and would then undergo a smooth transition to the rectangular form of the cathode.

The result presented has still some minor inconsistencies but is believed to be a good approximation to the actual case. Some spot checks were made by calculation donsidering the anode to be charged and taking into account the eight image charges in the cathode.

It is concluded that the field is very similar to that in a counter having cylindrical electrodes up to a radius comparable with the cathode size.
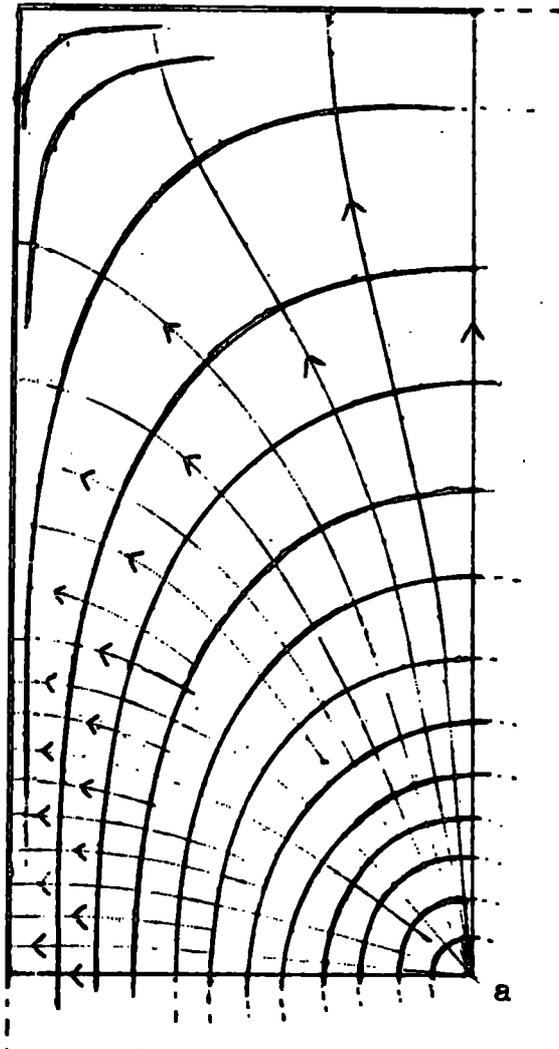
Fig. A.1.1. Field in the Proportional Counter
(showing equipotentials and
lines of electric intensity)

Anode is at a.

b) Operating Voltage.

Rosse and Staub (1949) show for cylindrical counters

$$M = f \left(\frac{V}{\ln \frac{b}{a}}, pa \right)$$

Where M = multiplication

V = operating voltage

b = cathode radius

a = anode radius

p = operating gas pressure

They argue that for a given value of M that the conditions in the critical region close to the wire must remain identical for multiplication purposes, i.e. for a given pressure the field near the wire (at a distance $r \frac{V}{r \ln(\frac{b}{a})}$) should be constant, and if the pressure is varied then a & b should also be changed in the inverse ratio so that the energy gained between collisions and the number of collisions in the critical region remain unaffected.

West (1953) has published results on the variation of M with operating voltage for various pressures of argon and using the expression of Rosse and Staub quoted above it can be shown that the simplest expression for M applicable to these resutls is

$$M = A \exp \left(\frac{V}{\ln \frac{B}{a}} \quad \frac{1}{pa} \right)$$

for 10 < M < 1000

This result may be expected to be generally true.

Finally, it is relevant to note that the operating voltage for neon is abnormally low compared with other gases.

APPENDIX II
THE RADIOACTIVE SOURCES.

a) Nature of the Sources

Both of the radioactive sources used, Zn^{65} and Sn^{113}, have as a major percentage of their decay schemes electron capture (EC) Xrays characteristic of the daughter element are then emitted. The sources are chosen for the suitability of the X-ray energy for this experiment, for their relatively long half-lives, and the lack of other decay products which might produce effects in the counter. The source characteristics are detailed in Table 1.

b) Results obtained with the Sources.

i) Ratio of the pulse heights produced by the sources.

The ratio of the mean pulse heights was 2.98 ± 0.05 showing agreement with the theoretical value within experimental error. From this we may conclude that the proportional counter is not saturating over the range of ion-pair production of interest in this experiment.

ii) The pulse height distribution produced by the sources.

A typical pulse-height distribution for the zinc source is shown in Fig. A 2.1, both as recorded (with cosmic ray background) and with the background subtracted. As predicted by theory the distribution is symmetrical. The distributions for the tin source were similar but with a lower percentage width.

iii) The dependence of pulse height on the E.H.T. applied to the counter.

In the course of investigating the performance of the proportional counter the pulse heights produced by one source were found for different values of the E.H.T. (which was available in ~ 95v steps) applied to the counter. Three of the results about the normal operating voltage (1050v) are shown in Fig. A2.2. These three only have been

RADIOACTIVE SOURCES.

Zn^{65}

Half life 245 days

Type of Radiation   EC β γ +

Energy in Mev   EC* (98.5%)   1.11 (45%)

                     β + 0.325 (1.5%)

* Emits characteristic Cu X-rays 8.0 kev.

\+ Two 0.51 Mev γ - rays are emitted when a positron is stopped.

Sn^{113}

Half Life 119 days

Type of Radiation EC* γ IC

Energy in Mev   100%   0.39(67%) 33%

* Emits characteristic In x-rays 24 kev and 3.3 kev.

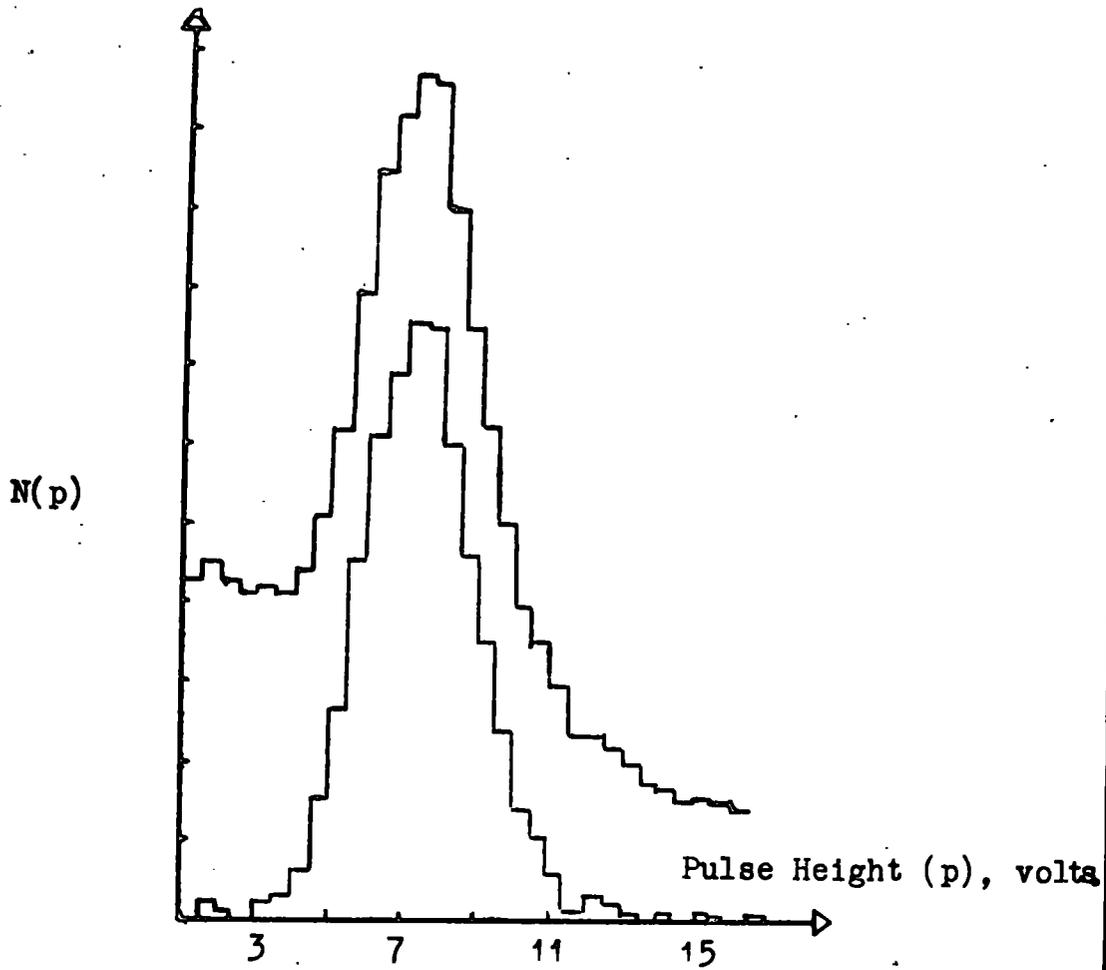Table 1.

Radioactive Sources

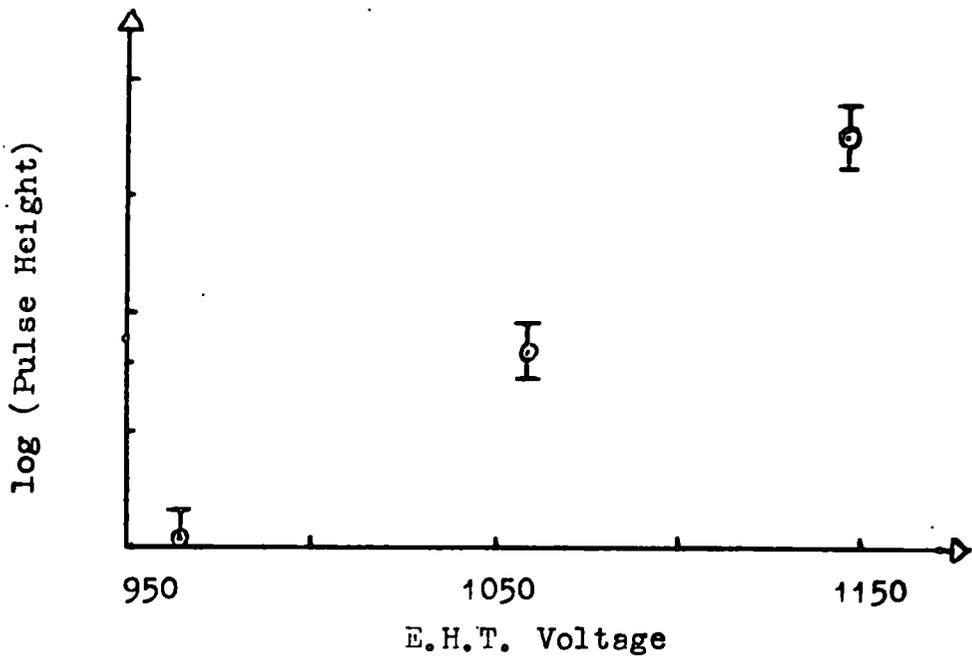Fig. A.2.1 Pulse Height Distribution, Zn Source

Fig. A.2.2 Variation of Amplification with E.H.T.

included since these were the only three that came within the normal range of the recording apparatus without changing the settings of the main amplifier.

The logarithm (base 10) of the pulse height is plotted against E.H.T. The results are consistent with a linear relationship between these quantities.

Now from this graph we can get

$$\frac{d(\ln p)}{dV} \qquad \text{where } p = \text{pulse height}$$
$$V = \text{E.H.T volts.}$$

$$\text{Taking } \ln p = K \log_{10} p.$$

$$\text{but } \frac{dp}{dV} = \frac{dp}{d(\ln p)} \cdot \frac{d(\ln p)}{dV}$$

$$\text{ie } \frac{dp}{dV} = p \frac{d(\ln p)}{dV}$$

$$= K p \frac{d(\log p)}{dV}$$

giving the results quoted in Chapter 9.

iv) The widths of the distributions.

Values for the half height, full width of several Zn distributions range between 17·5 $\pm$ 0·5% and to 20 $\pm$ 1% The average value may be taken as 19·0 $\pm$ 0·5%.

The values for the tin sources, except in one case where the width was 10·5 $\pm$ 0·5% range between 11% and 12% averaging about 11·5 $\pm$ 0·5%.

Theory (Chapter 8) shows that the width of the distribution is inversely proportional to the square root of the number of primary electrons released in the counter. The ratio of the numbers released by Sn and Zn will be the same as that of their energies i.e. 3 : 1.

Thus we would expect the ratio of the distribution widths to be 1 : 1.7.

In fact it can be seen that the ratio is 1·65 ± 0·05, a close agreement, though it must be remembered that the experimental values will include some width, due to the amplifier system, which may be expected to affect the ratio slightly.

The standard deviation (σ) may be found by dividing the full widths by 2·36. The resulting values are somewhat more than expected by theory (Chapter $\mathcal{S}$) but agree well with the results of West (1953).

The widths corresponding to the pulse heights for different values of E.H.T. were as follows:-

Pulse Heights (volts)	Width
2·5	20 ± 5%
8·0	19 ± 2%
27·0	20 ± 1%

These results suggest that, as theory predicts, the fractional width does not depend on the amplification factor within the counter.

c) Conclusions.

The results given above indicate that the counter is behaving normally.

APPENDIX. III

CALCULATION OF THE THEORETICAL IONIZATION LOSS IN NEON AND METHANE.

i) Landau Equation and its Modification.

The result given by Landau's theory for the most probable energy loss (Δ_0) in a single component absorber is

$$\Delta_0 = \xi \left(ln \frac{\xi}{\underset{\sim}{}} + 0.37 \right)$$

where

$$\xi = \frac{2\pi N}{mv^2} \rho \frac{Z}{A} x$$

and

$$ln \underset{\sim}{} = ln \frac{(1-\beta^2) I^2}{2mv^2} + \beta^2$$

where x is the thickness in cm. and other symbols have conventional meanings.

Using $I = I_0 Z$ ($I_0 = 13.5$ev) Landau rearranges the equation to give

$$\Delta_0 = \xi \left[ln \frac{3000 \beta^2 \xi}{Z^2(1-\beta^2)} + 1 - \beta^2 \right] ev$$

where

$$\xi = \frac{1.54 \times 10 \xi \cdot x}{\beta^2} \frac{Z}{A} \; e.v$$

Sternheimer (1956) after considering the results of Caldwell (1955) and Sachs and Richardson (1953) prefers $I = 13.0Z$ev

Then

$$\Delta_0 = \xi \left[ln \frac{3231 \beta^2 \xi}{Z^2(1-\beta^2)} + 1 - \beta^2 \right]$$

ii) Calculation of ξ for Neon and Methane.

The counters are filled with 40.1 cm. Hg. of Neon and 2.8 cm. Hg. of Methane. Calculations for these two gases were performed for these pressures and also for each at one atmosphere pressure. Comparison between the values at the latter pressure was made in order that the filling might be treated as 43 cm. Hg. of neon only if they were similar. However, it was found that the two gases behave quite differently in their ability to stop the particle. The values of ξ in each case are given below

Values of ξ

a) Neon

Density of neon at N.T.P. = 0.0009 gm/cc.

The containers were filled at 20°C approx. and at a pressure of $40\cdot1$ cm. Hg.

Then taking $x = 4\cdot30 \times 2\cdot54$ cm.

$$Z = 10$$
$$A = 20\cdot183$$

$$\zeta_{Ne} = \frac{3\cdot686 \times 10^2}{\beta^2} \text{ ev.} \quad (40\cdot1 \text{ cm. Hg.})$$

also $$\zeta_{N_i} = \frac{7498 \times 10^2}{\beta^2} \text{ ev.} \quad (76 \text{ cm. Hg.})$$

b) Methane

Density of methane at N.T.P. $= 0\cdot0007167$ gm/cc.

$$Z = 10$$
$$A = 16\cdot03$$

Giving $$\zeta_{CH_4} = \frac{7\cdot520 \times 10}{\beta^2} \text{ ev.} \quad (76 \text{ cm. Hg.})$$

and $$\zeta_{CH_4} = \frac{2\cdot673 \times 10}{\beta^2} \text{ ev.} \quad (2\cdot8 \text{ cm. Hg.})$$

Although ζ_{Ne} and ζ_{CH_4} are similar Δ_{Ne} and Δ_{CH_4} are not, the difference being due to the logarithmic term of the expression for Δ_o. Here the effective value of Z for methane had to be calculated.

(Defining effective $Z = \frac{I}{I_0}$)

Sternheimer gives I for methane in Rydberg units.

Now $I = \alpha R$ cm.$^{-1}$ where α is a constant for a substance.

Thus $I = \frac{\alpha Rhc}{K}$ ev.

where $K = 1\cdot6021 \times 10^{-13}$

For methane $I = 3\cdot27$ Rydberg units.

$$= 44\cdot47 \text{ ev.}$$

Effective Z $= 3\cdot421$

iii) Calculation for a gas mixture

If $\eta = \beta^2 \zeta$ and Δ_i is the loss in component i given by

$$\Delta_i = \frac{\eta_i}{\beta^2} \left[\ln \frac{3231\eta}{Z_i^2(1-\beta^2)} + 1 - \beta^2 \right]$$

and
$$\eta_i = \frac{2\pi N e^4 \rho_c \sum Z_i}{m v^2 \sum A_i} x_-$$

where $\eta = \sum \eta_i$ for the mixture,

then the most probable energy loss in the mixture (Δ) is given by

$$\Delta = \sum \Delta_i$$

An expression for energy loss in each component by itself
had already been calculated $(\Delta_i = \xi_i [F(\eta_i)])$

The correct value $\Delta_i = \xi_i [F(\eta)]$

was found by $\Delta_i = \xi_i \left[F(\eta_i) + \ln\left(\frac{\eta}{\eta_i}\right) \right]$

iv) The Density Effect δ

From the Sternheimer treatment

$$\left(\frac{\partial E}{\partial x}\right) = \frac{2\pi n e^4}{m v^2} \left[\sum_i f_i \frac{l_i^2 + l^2}{l_i^2} - l^2(1-\beta^2) \right]$$

where l satifies
$$\frac{1}{\beta^2} - 1 = \sum_i \frac{f_i}{\overline{v}_i^2 + l^2}$$

f = oscillator strength for the i'th transition

$l_i = (\overline{v}_v^2 + f_i^2)^{\frac{1}{2}}$

$\overline{v}_i$ = energy of the transition in units of $h v_p$

where
$$v_p = \left(\frac{n e^2}{\pi m}\right)^{\frac{1}{2}}$$

This may be applied to a mixture by calculating v_p for the total
number of electrons.

In this experiment however, the density effect in the region
of interest would be small, and the error in assuming this effect to be
due to 43 cm. Hg. of neon would be small. Thus advantage was taken of
Sternheimer's analytical expression for δ.

$$\delta = 4.606X + C + a(X_1 - X)^m \quad (X_0 < X < X_1)$$
$$= 4.606X + C \quad (X > X_1)$$
where $X = \log_{10}\left(\frac{p}{\mu c}\right)$

The other symbols are constants which very with the substance under consideration and have the following values for neon

$$C = -11 \cdot 72$$
$$a = 0 \cdot 258$$
$$m = 3 \cdot 18$$
$$X = 4$$
$$X = 2 \cdot 14$$

Note that the density effect thus starts to occur at a momentum given by $\dfrac{p}{\mu c} = 10^{X_0}$

The expression refers to a gas at atmospheric pressure and at a different pressure the correction is given by $\delta_A(p') = \delta_1(pA^{-\frac{1}{2}})$, where $\delta_A(p')$ is the correction at momentum p' for a pressure of A atmospheres.

Taking all these factors into account the onset of the density effect occurs at 19·4 Gev/c for the counters used in the experiment.

The values given by the analytical expression for δ must be modified before they can be used to correct the energy loss values since these values for δ are intended for Sternheimer's form of energy loss equation.

The value to be subtracted here δ_L is given by
$$\delta_L = \frac{A \rho x}{\beta^2} \cdot \delta \; \text{Mev}.$$
where A is a constant.

v) Cerenkov Radiation

In view of the lack of theoretical agreement over the magnitude of the energy loss in the form of Cerenkov radiation, no account was taken of it in calculating the expected energy loss. It was considered small enough to neglect.

vi) N on-participation of K-electrons

The value of ζ for neon in this experiment is 350-400 ev. in the relativistic region. The ionization potential of the K electrons is 864 ev. Hence these electrons are unlikely to participate in the most probable energy loss.

This will have a double effect on the calculation of the energy loss, given by

$$\Delta_0 = \frac{\zeta}{\beta^2} \left[F \left(\ln \frac{\zeta}{(I_0 Z)^2} \right) \right].$$

ζ will be reduced to $\frac{\zeta}{10}$ of its value, and if $I_0 Z$ is taken as the ionization potential of the L electrons (54v) then the logarithmic function will be increased

$$\left(\frac{130}{54} \right)^2 \times \frac{8}{10} \text{ times}$$

i.e. to the term in the bracket must be added

1n4.64

Thus if the log-rise region of the curve is represented by the ration,

$$\frac{\text{Ionisation at p = 10 Gev/c}}{\text{Ionization at p = 1 Gev/c}} = \frac{I_{10}}{I_0}$$

Then calculation shows that, if the K electrons are excluded

$$\frac{I_{10}}{I_0} = 1 \cdot 30 \frac{\zeta_{10}}{\zeta_1} = 1 \cdot 325$$

and if K electrons are included

$$\frac{I_{10}}{I_0} = 1 \cdot 33 \frac{\zeta_{10}}{\zeta_1} = 1 \cdot 315$$

The experimental results show that

$$\frac{I_{10}}{I_0} = 1 \cdot 290 \pm 0 \cdot 015$$

The accuracy not being quite high enough to exclude either theoretical value.

Calculations also show that if the K electrons are excluded the actual energy loss drops to between 89% (at 1 Gev/c) and 87% (at 10 Gev/c) of the value including them.

As indicated elsewhere, it was not considered possible in this experiment to get absolute values for the ionization loss, but if the necessary assumptions (Chap. 9) are valid then the experimental values are about 90% of those calculated. The error is indeterminate

and likely to be large but not so as to escape the conclusion that the experimental values are probably lower than those given by theory.

vii) Conclusions

We may conclude then that the experimental values agree well with values calculated using Landau's equation and that the agreement is better if the K electrons of neon are considered not to contribute to the most probable energy loss of the μ-mesons.

REFERENCES.

Alikhanov, A.I., Lubimov, V.A., and Eliseiev, G.P.,
        1956, Cern Symposium

Ashton, F., Brooke, G., Gardener, M., Hayman, P.J., Jones, D.G.,
Lloyd, J.L., Taylor, F.E., West, R.H., and Wolfendale, A.W.,
        1960, Nature, 185 No. 3710, 364 - 365.

Bakker, C.J., and Segre, E., 1951, Phys. Rev., 81, 489.

Barnaby,   1960, Private Communication.

Behrens, D.J., A.E.R.E. Reports T/M 50.

Bethe, H.A., 1930, Ann. Phys. Lpz., 5,325;
        1932, Z. Phys., 76, 293;
        1933, Handbuch der Physik, 24, 515.

Bhabha, H.J., 1937, Proc. Roy. Soc.A. 164, 257.

Bloch, F., 1933a, Ann. Phys., Lpz., 16, 285;
        1933b, Z.Phys., 81, 363.

Bisi, A., and Zappa, L., 1955, Nuovo Cim., 10.

Blunck, O., and Leisegang, S., 1950, Z. Phys., 128, 500.

Bohr, N., 1915, Phil. Mag., 30, 581.
        1948, Det. Kgl. Dans. Vid. Sels., 18, 8.

Bowe, J.C., 1960, Phys. Rev., 117, 1411.

Budini, P., and Taffara, L., 1953, Nuovo Cim., 10, 1489;
        1956, Nuovo Cim.,

Caro, D., Parry, J., and Rathgeber, H., 1951, Aust. J. Sci. Res., A, 4, 16.

Caldwell, D., 1955, Phys. Rev., 100, 201.

Curran, S.C., and Craggs, J., 'Ionization Chambers'

Curran, S.C., Proportional Counters Handbuch der Physik XLV.

Eyeions, D.A., Owen, B.G., Price, B.T., and Wilson, J.G.,
        1955, Proc. Phys. Soc., A., 68.

Fano, U., 1947, Phys. Rev., 72, 26;
        1953,Phys. Rev., 92, 328.,
        1956, Phys. Rev., 103, 1,202.

Fermi, E., 1939, Phys. Rev., 56, 1242;
        1940, Ibid., 57, 485.

Fortune, R., 1960, Ph.d. Thesis Berne.

Fowler, G.N., and Jones, G.M.B.D., 1953, Proc. Phys. Soc., A., 66, 597.

Frank, I., and Tamm, I., 1937, C.R.Acad. Sci. U.S.S.R., 14, 109.

Ghosh, S.K., Jones, G.M.B.D., and Wilson, J.G., 1952, Proc. Phys. Soc. A.
        65, 68; 1954, Ibid., 67, 331.

Gooding, A., and Eiseberg, R.M. 1957, Phys. Rev., 105, 357.

Hall, G., 1959, Canad, J. Phys. 37, 2,189.

Halpern, O., and Hall, H., 1940, Phys. Rev., 57, 459;
                1948, Ibid., 73, 477.

Hammersley, J.M. and Morton, K.W., 1954, Biometrika, 41, 296.

Hines, K.C., 1955, Phys. Rev., 97, 1725.

Huybrechts, M., and Schonberg, M., 1952, Nuovo Cim., 9,764.

Hyams, B.D., Mylroi, M.G., Owen, B.G., and Wilson, J.G.,
        1950, Proc. Phys. Soc. A., 63, 1053.

Hussein, I., and Jaffe, D., 1959, Nucl. Inst. and Meth., 6,195.

Igo, G., and Eiseberg, R.M., 1954, Rev. Sci. Inst., 25, 304.

Kepler, R.G., D'Aundlau, C.A., Fretter, W.B., and Hansen, L.F.,
        1958, Nuovo. Cim., X,7, 71.

Lagarrigue, A., Musset, P., Rancon, P., Sauteron, X and Rousset, A.,
        1959, Nuovo Cim., XIV, 2,370.

Landau, L., 1944, J. Phys. U.S.S.R., 8,201.

Lanou, R.E., and Kraybill, H.L., 1959, Phys. Rev., 113,657.

Moller, C., 1932, Ann. Phys., Lpz., 14, 531.

Moyal, ., 1955, Phil. Mag., 46.

Mylroi, M.G., and Wilson, J.G., 1951, Proc. Phys. Soc., A., 64, 404.

Owen, B.G., and Wilson, J.G., 1955, Proc. Phys. Soc. A, 68, 409.

Palmatier, E.D., Meers, J., Askey, K., 1955, Physics. Rev., 97, 486.

Price, B.T., West, D., Becker, J. Chanson, P., Nageotte, E., and Treille, P.,
        1953, Proc. Phys. Soc., A., 63, 167.

Price, B.T., 1955, Rep. Prog. Phys., XVIII, 52.

Rosenweig, W., 1959, Phys. Rev., 115, 1683.

Rossi, B., and Staub, I., 1950, "Ionization Chambers and Counters". (McGraw-Hill).

Rothwell, P., and West, D., 1950, Proc. Phys. Soc. A., 63,539.

Sachs, D.C., and Richardson, R.J., 1951, Phys. Rev., 83.
1953, Phys. Rev., 89, 1163.

Sternheimer, R.M., 1952, Phys. Rev., 88, 851;
1953a, Ibid., 89, 1148;
1953b, Ibid., 91, 256;
1954, Ibid., 93, 735;
1956, Ibid., 103, 511.

Swan, W.F.G., 1938, J. Franklin Inst. 226, 598.

Symon, K.R., 1948, Thesis, Harvard University, some of which is reproduced in "High Energy Particles" by Rossi.

Tidman, D.A., 1956, Nucl. Physics. 2 and 4.

Valentine, J.M., and Curran, S.C., 1952, Phil. Mag., 43,964.
1958, Rep. Prog. Phys.

Vavilov, P.V., 1957, J.E.T.P., 5,749.

Walske, M.C., 1956, Phys. Rev., 101.

West, D., 1953a, Proc. Phys. Soc. A., 66, 306;
1953b, "Progress in Nuclear Physics", 3 (London Pergamon Press)

Wick, G.C., 1940, Ric. Scient., 11,273.
1943, Nuovo Cim., 1,302.

Williams, E.J., 1929, Proc. Roy. Soc. A., 125,420;
1931, Ibid., 130,310.